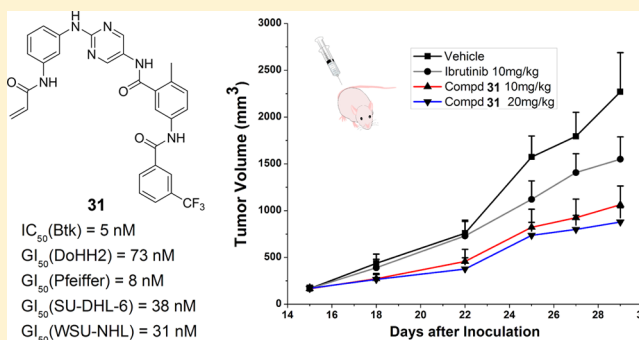


Discovery of a Series of 2,5-Diaminopyrimidine Covalent Irreversible Inhibitors of Bruton's Tyrosine Kinase with in Vivo Antitumor Activity

Xitao Li,[†] Yingying Zuo,[†] Guanghui Tang,[†] Yan Wang,[†] Yiqing Zhou,[†] Xueying Wang,[†] Tianlin Guo,[†] Mengying Xia,[†] Ning Ding,[‡] and Zhengying Pan^{*,†}[†]Key Laboratory of Chemical Genomics, Key Laboratory of Structural Biology, School of Chemical Biology and Biotechnology, Shenzhen Graduate School, Peking University, Shenzhen, 518055, China[‡]Key Laboratory of Carcinogenesis and Translational Research (Ministry of Education), Department of Lymphoma, Peking University Cancer Hospital and Institute, No. 52 Fucheng Road, Haidian District, Beijing, 100142, China

S Supporting Information

ABSTRACT: Bruton's tyrosine kinase (Btk) is an attractive drug target for treating several B-cell lineage cancers. Ibrutinib is a first-in-class covalent irreversible Btk inhibitor and has demonstrated impressive effects in multiple clinical trials. Herein, we present a series of novel 2,5-diaminopyrimidine covalent irreversible inhibitors of Btk. Compared with ibrutinib, these inhibitors exhibited a different selectivity profile for the analyzed kinases as well as a dual-action mode of inhibition of both Btk activation and catalytic activity, which counteracts a negative regulation loop for Btk. Two compounds from this series, **31** and **38**, showed potent antiproliferative activities toward multiple B-cell lymphoma cell lines, including germinal center B-cell-like diffuse large B cell lymphoma (GCB-DLBCL) cells. In addition, compound **31** significantly prevented tumor growth in a mouse xenograft model.



■ INTRODUCTION

The B-cell receptor (BCR) signaling pathway plays an important role in B-cell development and differentiation.^{1,2} Bruton's tyrosine kinase (Btk) is a crucial component of the BCR pathway and is expressed only in hematopoietic cells except natural killer or T cells.³ Patients with X-linked agammaglobulinemia, which is a rare genetic disease resulting from mutations in Btk, exhibit a reduced number of mature B-cells.^{4,5} Btk has also been linked to chronic BCR activation in activated B-cell-like diffuse large B cell lymphoma (ABC-DLBCL), which is a critical factor in the promotion of lymphoma cell survival.^{6,7}

Since Btk was discovered in the 1990s, multiple Btk inhibitors have been developed.^{8,9} These inhibitors can be divided into two major classes, reversible and covalent irreversible ones (Figure 1). LFM-A13,¹⁰ dasatinib,¹¹ **1** (CGI-1746),¹² **2** (GDC-0834),¹³ and RN-486^{9,14} are reversible Btk inhibitors. These inhibitors have shown potent effects for immune disorders in multiple animal models, and **2** has been advanced into a phase I clinical trial. Ibrutinib¹⁵ from Celera/Pharmaceuticals/Janssen and **3** (CC-292)¹⁶ from Celgene and the imidazoquinoxaline compounds¹⁷ from Pfizer are the primary examples of covalent irreversible Btk inhibitors. Ibrutinib and **3** are currently in multiple clinical trials, and ibrutinib was just approved to treat patients with mantle cell lymphoma in November 2013. Both compounds interact with a cysteine residue (Cys481) located at the rim of the ATP-binding pocket in Btk. These types of irreversible Btk inhibitors have unique characteristics compared with traditional reversible ones,

such as a long drug–target residence time and the decoupling of pharmacokinetic and pharmacodynamic properties.¹⁸ Btk inhibitors have been shown to be highly efficacious in animal models of rheumatoid arthritis, lupus, and lymphoma;^{19,20} multiple clinical trials of ibrutinib and **3** have also shown encouraging results in patients.^{21,22} Therefore, developing Btk inhibitors is a promising strategy to treat overactive B-cell diseases such as autoimmune disorders and lymphoma.

Targeted covalent drugs have recently garnered significant interest, particularly for kinase inhibitors.^{23–25} Since the pioneering work on EGFR/HER2 inhibitors,^{26–28} in addition to Btk, selective covalent inhibitors have been developed for Bmx,²⁹ FGFR,³⁰ GSK3 β ,³¹ Itk,³² JNK,³³ Kit/PDGFR,³⁴ Nek2,³⁵ PI3K α ,³⁶ RSK,³⁷ and Src family kinases.^{38,39} This field has also been discussed in several excellent reviews.^{40,41} Covalent bond formation between the inhibitors and nonconserved cysteine residues proximal to the ATP binding pockets of the kinase catalytic domain enhances the potency and selectivity of this type of inhibitor. We use a two-step procedure to develop such inhibitors. In the first step, we optimize the template without covalent reactive groups. In the second step, structural information is used to guide the placement of a reactive group at a suitable position on the parent template to enable an interaction with the sulfhydryl group of the targeted cysteine. After the first step,

Received: November 16, 2013

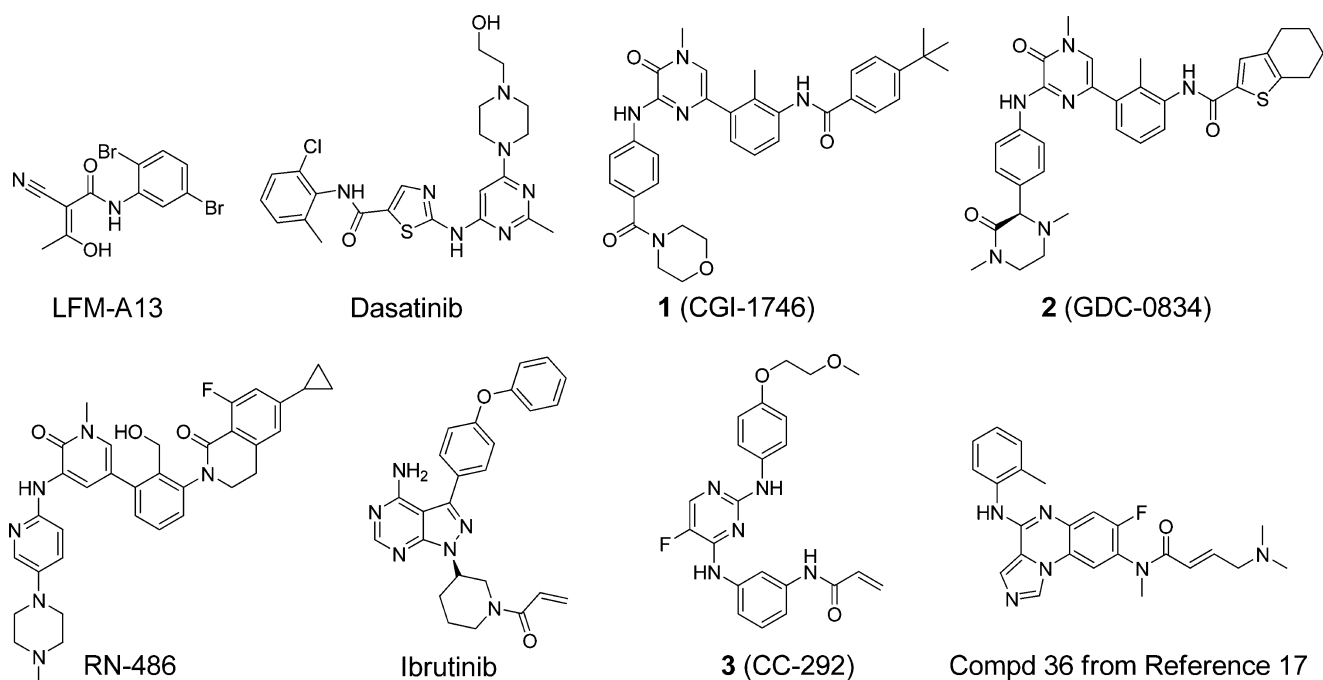


Figure 1. Examples of Btk inhibitors.

we select compounds reaching low nanomolar potency, which often suggest that the template substantially interacts with the target kinase, thus facilitating the selection of reactive groups in the second step. In the second step, a mild reactive group is typically preferred to limit the off-target effects that would result from indiscriminate reactions with other cellular nucleophiles.

In cells, Btk is first activated by its upstream kinases through phosphorylation of a key tyrosine residue (Tyr551), which increases the catalytic activity of Btk by 10-fold.⁴² Following autophosphorylation of another tyrosine residue (Tyr223), Btk becomes fully activated and phosphorylates its substrates, such as PLC- γ 2 in the BCR pathway.⁴³ Btk is an efficient enzyme; only a small fraction of existing Btk is activated, and approximately 30 min of Btk activity is required for full signal transduction along the BCR pathway.⁴⁴ In vivo studies also indicate that more than 60% of Btk activity must be inhibited to achieve observable efficacy in animal models.⁴⁵ Thus, an irreversible inhibitor with a long drug–target residence time would be preferable for sustained Btk inhibition. In addition, Btk is also influenced by a negative feedback loop in the BCR pathway. The kinase PKC β is downstream of Btk in the BCR pathway, and it has been suggested that PKC β directly and negatively regulates Btk activity by impeding Btk's engagement with the signaling complex.⁴⁶ Treating Namalwa cells with ibrutinib increases Tyr551 phosphorylation, the first step in Btk activation, suggesting the existence of Btk-mediated negative feedback loop.⁴⁷ It has been suggested that enhanced kinase activation is a potential resistance mechanism that cells adopt to overcome the effects of inhibitors.^{48–50} Multiple p38 kinase inhibitors have shown only transient activity in clinical trials.⁵¹ However, a dual-action p38 kinase inhibitor that prevents both the activation and kinase activity of p38 in cells, 4-(5-(cyclopropylcarbamoyl)-2-methylphenylamino)-5-methyl-N-propylpyrrolo[1,2-f][1,2,4]triazine-6-carboxamide (BMS-582949), has shown clinical efficacy in a phase IIa rheumatoid arthritis trial without tachyphylaxis.^{52,53} Inspired by this observation, we sought scaffolds with a dual-action mode that could prevent Btk Tyr551 from being

phosphorylated and also inhibit Btk's own catalytic ability. Developing such a dual-action mode Btk inhibitor that inhibits both Btk activation and catalysis could be a concise and effective strategy to further down-regulate BCR and other signal transduction pathways in which Btk plays an important role and to overcome potential resistance mechanisms due to increased Btk activation.

Herein, we present the first series of dual-action mode Btk covalent irreversible inhibitors based on a type II scaffold. These compounds are potent Btk inhibitors with high selectivity and have demonstrated significant antiproliferation activities in a mouse xenograft model of human B-cell lymphoma (DoHH2).

■ STRUCTURE-BASED DESIGN OF COVALENT BTK INHIBITORS

Kinase inhibitors can be categorized based on the kinase conformation that they recognize.⁵⁴ Type I kinase inhibitors (e.g., erlotinib and dasatinib) bind their target kinases in the active conformation, whereas type II inhibitors (e.g., imatinib and sorafenib) bind kinases in the inactive conformation. Because one of our goals is to prevent Btk activation, type I inhibitors that bind kinases in the active conformation may not be suitable; thus, we focused our efforts on type II inhibitors. Btk shares high sequence similarity with the Src family kinase Lck. We identified only one single amino acid difference between Btk (Cys481) and Lck (Ser323) within the direct contact range for analogues of ibrutinib.¹⁵ In addition, the literature has suggested the existence of cross-reactivity for many Btk and Lck inhibitors.^{11,15,55} Thus, we hypothesized that known type II Lck inhibitors would provide useful insights regarding the design of novel Btk inhibitors; therefore, we used the 2,5-diaminopyrimidine compounds developed by scientists at Amgen as a starting point.⁵⁶

A Btk crystal structure that adopts a DFG-out conformation (PDB code 3PJ3)⁵⁷ was used as a template for our design. The 2,5-diaminopyrimidine compound 4 was easily docked into this structure without obvious steric conflicts. As indicated in the

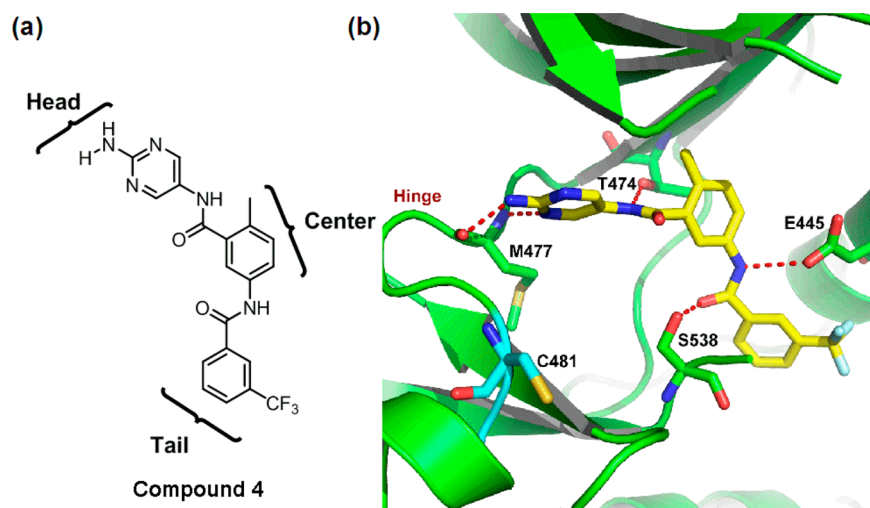


Figure 2. (a) Structure of compound **4** and the “head”, “center”, and “tail” regions in the structure–activity relationship (SAR) study. (b) Compound **4** (carbon atoms in yellow) was docked in a structure of Btk (PDB code 3PJ3). The red dots indicate potential hydrogen bonds between compound **4** and Btk. Cys481 (carbon atoms in cyan) is highlighted.

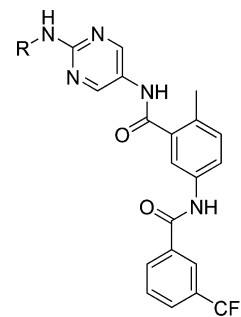
model, compound **4** could form several important hydrogen bonds with Btk, including with Met477 at the hinge region and the gatekeeper residue Thr474, as well as hydrogen bonds with Glu445 and Ser538. Compared to the conformation of its parent compound in Lck (PDB code 3BYU), compound **4** adopts an almost identical conformation and forms similar interactions with the protein. This model suggests that 2,5-diaminopyrimidine compounds have potential as inhibitors against Btk, but the selectivity between Btk and Lck might be difficult to achieve for this scaffold. However, because ibrutinib has demonstrated remarkable efficacy and safety in clinical studies even though it is a potent inhibitor of Lck, Lyn, and other Src family kinases, the selectivity between Btk and Lck was not a critical factor in our program.

RESULTS AND DISCUSSION

Structure–Activity Relationship. On the basis of our docking model, we divided the 2,5-diaminopyrimidine scaffold into head, center, and tail regions (Figure 2), which were then explored sequentially.

The head area is proximal to the hinge region in Btk, and the amino acid composition of this region is very similar between Btk and Lck; thus, the IC_{50} values for the first set of compounds were surprising (Table 1). Compound **4** yielded an IC_{50} of 149 nM against Lck but only 3.42 μ M for Btk, a 23-fold difference. Attaching an ethyl or cyclopropyl group at the R position (**5** and **6**) did not substantially improve the potency. A phenyl group (**7**) at this position improved the IC_{50} values for Btk and Lck to 133 and 7 nM, respectively. Our model suggested that Btk’s Tyr476 would form π – π interactions with the newly added phenyl group in inhibitor **7**. Thus, we hypothesized that tuning the electron density of the phenyl group might impact inhibitor potency. Decorating the phenyl group with an *m*-CF₃ group yielded a less potent inhibitor (**8**). Substitution with the electron-donating group MeO (**9**) improved potency for Btk. However, substitution with electron-withdrawing F (**10**) yielded an inhibitor with a potency equal to that of **9**. Fortunately, substituting an amino group at either the meta or para positions of the phenyl ring produced inhibitors with comparable nanomolar potencies against both Btk and Lck. In the absence of crystal structures for the inhibitor–kinase complexes, it is difficult to identify the exact basis for the

Table 1. Head Region SAR^a



Compd	R	IC ₅₀ (nM)	
		Btk	Lck
4	H	3423	149
5	Et	1106	142
6	Cyclopropyl	2153	ND
7	Phenyl	133	7
8	3-CF ₃ -phenyl	304	16
9	3-MeO-phenyl	53	4
10	3-F-phenyl	52	4
11	4-NH ₂ -phenyl	8	4
12	3-NH ₂ -phenyl	14	5
13		15	7
14		14	0.9
15		1410	287

^a IC_{50} values are reported as means of duplicates. ND, not determined.

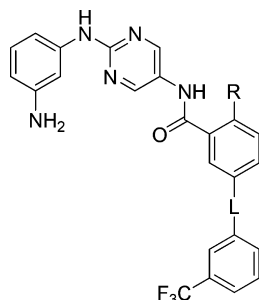
10-fold improvement (compounds **7**–**12**) in potency toward Btk but the largely flat SAR for Lck. This difference may be not only due to the identities of the amino acid residues that directly contact the inhibitors but also due to the overall plasticity of the

kinases in this region. Since the selectivity between Btk and Lck was not considered critical for our program, we did not explore this aspect of the inhibitors further.

The docking structure of compound **7** in the Btk cocrystal structure with a DFG-out conformation (PDB code 3PJ3) indicated that Cys481 is approximately 6–7 Å away from the phenyl ring at the head region of the inhibitors (Supporting Information Figure 1). We anticipated that the addition of a linker group extending from the meta position of this phenyl ring would yield substituents that could directly interact with the Cys481 sulfhydryl group. Acylating the *m*-amino group with simple acids (**13** and **14**) largely maintained the potency even though the bis-acylated compound **15** exhibited significantly reduced potency. These results indicate that it is possible to accommodate a substitution at the meta position.

Next, we probed the SAR at the central region (Table 2). The angular methyl group at the R position might fit snugly

Table 2. Center Region SAR^a



Compd	R	L	Btk IC ₅₀ (nM)
12	Me		14
16	Cl		11
17	F		47
18	H		233
19	Me		45
20	Me		63

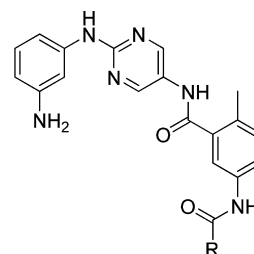
^aIC₅₀ values are reported as mean values of duplicates.

into a small hydrophobic pocket formed with the gatekeeper residue Thr474. Replacing this methyl group with a common bioisostere (Cl) yielded the equally potent compound **16**. Decreasing the sizes of substitution to F (**17**) and H (**18**) decreased the potency by 3- and 16-fold, respectively. The amide at the L position was expected to form hydrogen bonds with Glu445 and Ser538, which may be important for type II inhibitors. Reversing the amide group orientation (**19**) reduced the potency 3-fold for Btk, while a urea linkage (**20**) reduced the potency 5-fold; thus, an amide linkage was selected in the next SAR studies.

For type II inhibitors, we anticipated that tail region substitutions would occupy the hydrophobic pocket vacated

by the movement of the phenyl group of the phenylalanine residue in the “DFG” sequence. As expected, an aromatic group was required at the R position (Table 3) because compounds

Table 3. Tail Region SAR^a

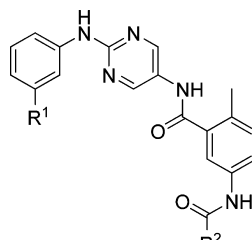


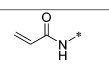
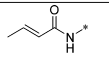
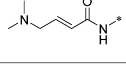
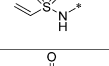
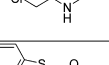
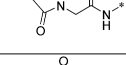
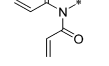
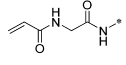
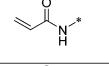
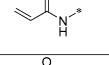
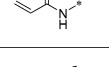
compd	R	Btk IC ₅₀ (nM)
12	3-CF ₃ -phenyl	14
21	Et	8563
22	cyclopropyl	4946
23	3-Cl-phenyl	20
24	3-NMe ₂ -phenyl	47
25	3-F-phenyl	166
26	3-Cl-5-CF ₃ -phenyl	18
27	4-Cl-3-CF ₃ -phenyl	9
28	4-CF ₃ -phenyl	25
29	styryl	24
30	2-naphthyl	39

^aIC₅₀ values are reported as means of duplicates.

with either ethyl (**21**) or cyclopropyl (**22**) groups exhibited significantly reduced potency, likely due to a significant decrease in hydrophobic interactions with the protein. However, various aromatic ring substitutions were generally tolerated. By use of the *m*-CF₃-substituted compound **12** as a benchmark, a chlorine substitution yielded an inhibitor (**23**) with comparable potency, a dimethylamino group (**24**) increased the IC₅₀ value by approximately 3-fold, and a fluorine atom (**25**) reduced the potency by more than 10-fold. A secondary chlorine substitution either meta or para to the amide did not significantly change the IC₅₀ values (**26** and **27**). Moving the CF₃ group to the para position (**28**) was well-tolerated, and compound **29**, which contained a styryl group, also had comparable potency. Introducing a naphthyl group at the R position (**30**) maintained the IC₅₀ at 39 nM. Collectively, these data suggest that Btk has a relatively large and plastic pocket in the tail region.

The above SAR studies (Tables 1–3) indicated that compound **12** was highly potent against Btk, and our model indicated that the meta position (R¹) is the preferred site for anchoring reactive groups (Table 4). Thus, **12** was used as the template to probe the interaction between the inhibitors and Cys481. A panel of potential covalent reactive groups was attached to the free amino group at the R¹ position. Because the apparent potency of irreversible inhibitors varies with the length of the preincubation time between the enzyme and inhibitors, the preincubation time in our kinase activity assays was kept constant at 10 min. Compound **31**, which includes the classic acrylamide group, yielded an IC₅₀ of 5 nM for Btk. Adding a methyl group to the terminal carbon of the acrylamide (**32**) reduced inhibitor potency, which was partially recovered through further substitution with a dimethylamino group at the allylic position (**33**), consistent with the trend observed for other covalent inhibitors of Btk and EGFR.^{15,58} The methyl group reduced the electrophilicity and increased the steric hindrance of

Table 4. Reactive Group SAR^a


Compd	R ¹	R ²	Btk IC ₅₀ (nM)
31		3-CF ₃ -phenyl	5
32		3-CF ₃ -phenyl	36
33		3-CF ₃ -phenyl	15
34		3-CF ₃ -phenyl	16
35		3-CF ₃ -phenyl	15
36		3-CF ₃ -phenyl	18
37		3-CF ₃ -phenyl	208
38		3-CF ₃ -phenyl	< 4.4
39		3-F-phenyl	48
40		4-Cl-3-CF ₃ -phenyl	11
41		2-Naphthyl	22

^aIC₅₀ values are reported as mean values of duplicates.

the Michael acceptor, which reduced the potency of compound 32 by 7-fold, while the dimethylamino group in compound 33 was proposed to form a hydrogen bond with the cysteine residue thiol group, thus enhancing its nucleophilicity.⁵⁸ The vinyl sulfonamide 34 and two additional compounds with good leaving groups (35 and 36) were also potent, but the potency of the bis-acetylated compound (37) was reduced by more than 40-fold compared with compound 31. Interestingly, compound 38, which includes a glycyl spacer, exhibited excellent potency that was below the detection limit of our Btk enzyme assay. With acrylamide as the reactive group, variations at the R² position yielded compounds 39–41, which were all potent inhibitors of Btk.

One concern regarding covalent kinase inhibitors is that they may react nonselectively with thiols other than the intended target in a physiological environment. We used glutathione (GSH), which is a tripeptide that is naturally abundant in cells, as a surrogate to investigate acrylamide reactivity toward free thiols. When compound 31 (100 μM) was incubated with 5 mM GSH in PBS buffer at pH 7.4 at 37 °C, no adducts between compound 31 and GSH were detected after 2 h, suggesting that the acrylamide group does not react indiscriminately with thiols.

On the basis of their exceptional potency toward Btk, compounds 31 and 38 were selected for further biological evaluations.

Compounds 31 and 38 Are Selective Covalent Inhibitors of Btk. The selectivity of compound 31 was first profiled against a panel of kinases that included representatives of major classes of kinases and those kinases that directly participate in the BCR pathway (Figure 3). At 0.5 μM, compound

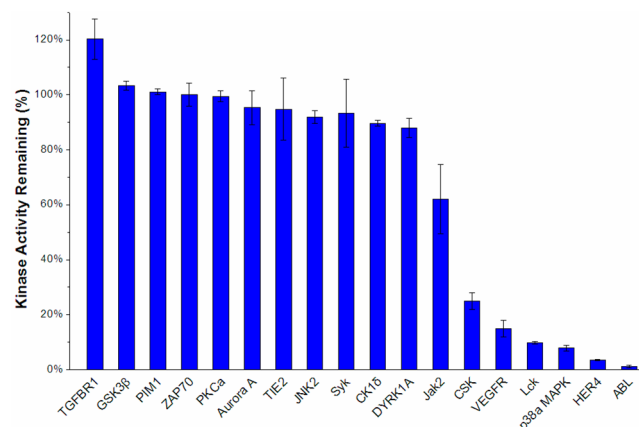


Figure 3. Selectivity of compound 31 against 18 kinases. The values are the mean of duplicates.

31 was inactive against the majority of the kinases tested and weakly active against Jak2. Compound 31 was moderately active against CSK but potentially inhibited ABL, HER4, Lck, p38α, and VEGFR. Type II inhibitors for ABL, p38α, and VEGFR kinases have been well-documented in the literature.^{59–63} Notably, the kinase selectivity of compound 31 was similar to that of ibrutinib for kinases that are directly involved in the BCR pathway, i.e., potent activity against Btk and Lck, which are representative Tec and Src family kinases, with no activity against Syk or PKC.

Reversible and irreversible inhibitors have different requirements for sustained inhibitory effects in cells.⁶⁴ Reversible inhibitors are in equilibrium with the biological target, whereas irreversible inhibitors bind continuously to the targeted protein until the protein is degraded through biological processes. Thus, reversible inhibitors must be maintained at a high enough concentration to suppress the target activity. However, irreversible inhibitors require only a high-concentration pulse to occupy the target binding sites and exert a sustained effect. In fact, irreversible inhibitors with short half-lives may be preferred to mitigate potential off-target effects. Thus, for covalent irreversible inhibitors, special attention should be paid to kinases that share a cysteine residue at the structurally identical position. Btk is among a group of 11 kinases out of more than 500 in the human kinome with a cysteine at the identical position (Cys481 in Btk). These kinases include Blk, Jak3, MAP2K7, Tec family (Bmx, Btk, Itk, Rlk, and Tec), and EGFR family (EGFR, HER2, and HER4) kinases. We measured the inhibitory effects of compounds 31 and 38 against 10 of these kinases (Table 5). They are quite potent against Blk, Bmx, Btk, Rlk, Tec, EGFR, HER2, and HER4. Notably, both compounds had weak activity against Jak3 in the micromolar range and no activity against Itk up to 30 μM. However, they were almost as potent as ibrutinib (5 nM) against EGFR. It is unclear whether this affinity for EGFR would produce major side effects in clinical studies. Also, caution should be taken when interpreting the selectivity of covalent inhibitors solely based on IC₅₀ values, as a recent study indicated that both reversible binding affinity and

Table 5. Selectivity against Kinases with a Cysteine Structurally Identical to Cys481 in Btk^a

compd	IC ₅₀ (nM)									
	Blk	Btk	Bmx	EGFR	HER2	HER4	Itk	Jak3	Rlk	Tec
31	2.7	5	1.9	11	19	5.5	>30 000	2680	1.9	8.2
38	4.2	<4.4	0.71	7	7	3.3	>30 000	6370	1.4	6.3

^aIC₅₀ values are reported as mean values of duplicates.

the chemical reactivity of these compounds can contribute separately to the overall biochemical potency.⁶⁵

Mass spectrometry was employed to determine whether compounds **31** and **38** formed covalent adducts with Btk. Incubating the Btk kinase domain with 3 equiv of each compound caused a complete mass peak shift, and the mass numbers for the new peaks were consistent with 1-to-1 complexes between the compounds and protein (Figure 4).

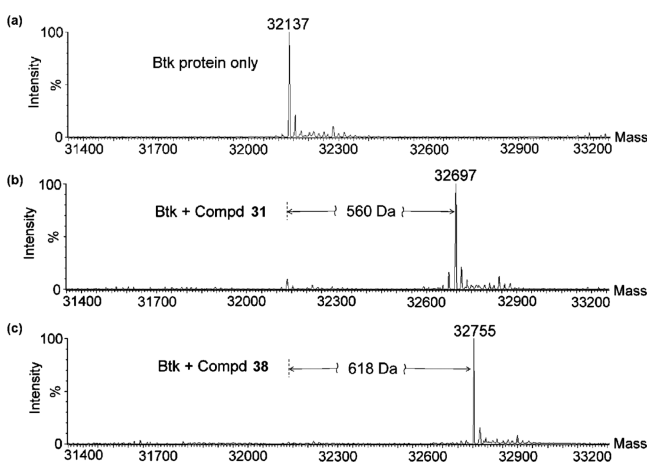


Figure 4. Mass spectra of the Btk kinase domain indicating that 1-to-1 adducts were formed between **31** or **38** and Btk. The molecular weight of apo Btk (387–659) is 32136. After incubation with **31** (exact mass, 560.5) or **38** (exact mass, 617.6) at 4 °C for 1 h, the peaks were fully shifted.

The adduct between compound **31** and Btk was digested with trypsin. Mass spectrometric analysis of the digested peptide fragments indicated that the modification site was, as expected, Cys481 (Supporting Information).

Compounds 31 and 38 Irreversibly Inhibit Btk Phosphorylation in Live Cells. In cells, BCR signaling is a graded process that is influenced by the convergence of both activating and negative regulatory events.⁴⁶ Upon BCR pathway activation, Btk moves to the cell membrane and is first phosphorylated at Tyr551 by upstream kinases. After an additional autophosphorylation step, Btk is fully activated and phosphorylates its physiological substrate, PLC- γ 2. Approximately 30 min later, Btk activity returns to the basal level through a negative feedback loop. PKC β , which is activated downstream of Btk, directly and negatively regulates Btk through Ser180 phosphorylation, which impairs Btk migration to the membrane and its overall phosphorylation/activation level.⁴⁶ Inhibiting Btk activity would interrupt downstream events in the BCR pathway, including the negative feedback loop, thus maintaining high Btk phosphorylation levels. Ibrutinib has been shown to augment Btk Tyr551 phosphorylation levels in Namalwa cells.⁴⁷ Among known Btk inhibitors, **1** binds the inactive conformation of Btk, in which Tyr551 is not phosphorylated. The crystal structure of Btk with **1**

(PDB code 3OCS) indicates that this compound extends into a deep pocket formed by Phe413, Leu542, Val546, and Tyr551, resulting in the movement of Tyr551 away from the solvent accessible area such that it may be unavailable for phosphorylation by upstream kinases.¹²

To test the inhibition mode of action of compounds **31** and **38**, we measured their abilities to inhibit the BCR pathway by monitoring the phosphorylation levels of Tyr551 in Btk and Tyr1217 in the Btk substrate PLC- γ 2. Both compounds strongly inhibited both phosphorylation events in live Ramos cells. Compounds **31** and **38** exhibited IC₅₀ values of 14 and 13 nM, respectively, for Btk Tyr551 phosphorylation and IC₅₀ values of 8.5 and 13 nM, respectively, for PLC- γ 2 Tyr1217 phosphorylation. In comparison, racemic version of ibrutinib (compound **4** in ref 15) inhibited PLC- γ 2 phosphorylation only, with an IC₅₀ of 14 nM, and showed virtually no inhibition (>7.5 μ M) of Btk Tyr551 phosphorylation. Thus, compounds **31** and **38** clearly exhibit a dual-action mode of inhibition in live cells.

Next, washout experiments were performed to confirm irreversible bond formation between Btk and the inhibitors in live cells (Figure 5). The acrylamide-containing compounds **31**

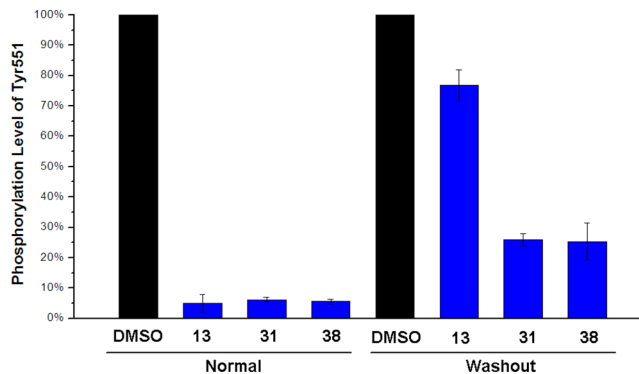


Figure 5. Washout experiments with the reversible inhibitor **13** and irreversible inhibitors **31** and **38**. In Ramos cells, Btk Tyr551 phosphorylation was measured after the cells were treated with compound for 1 h in a normal experiment or after treatment for 1 h followed by washout with fresh media for 2 h in the washout experiment.

and **38** maintained their inhibitory effects in cells even after a 2 h washout with fresh media, whereas Btk phosphorylation levels were largely restored in cells treated with the reversible analogue **13**, which contains a simple propylamide group, after removal of the compound. These data showed that both compounds **31** and **38** are irreversible inhibitors.

Antiproliferative Activities. Initial testing of compound **31** at two concentrations (1 and 10 μ M) against multiple non-Hodgkin's lymphoma and leukemia cell lines indicated that this compound was active in preventing the growth of these cancer cells (Figure 6). Cell viability assays further confirmed the initial results. Both compounds **31** and **38** displayed single-digit

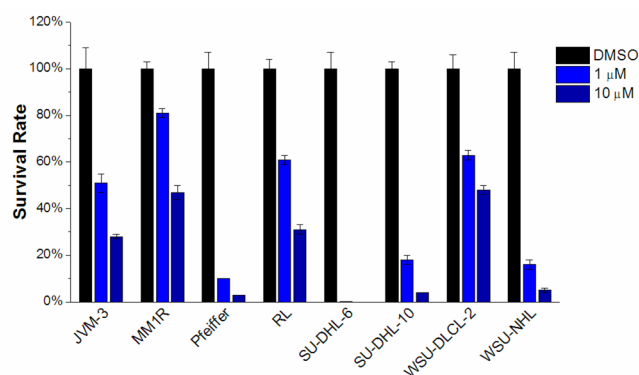


Figure 6. Compound **31** is a potent inhibitor of proliferation in multiple malignant B cell lines. The values shown are the averages of triplicates.

nanomolar potency in Pfeiffer cells and better efficacy than ibrutinib in DoHH2 cells with GI_{50} values of 73 nM (**31**) and 40 nM (**38**), respectively (Figure 7). SU-DHL-6 and WSU-NHL are two germinal center B-cell-like diffuse large B cell lymphoma (GCB-DLBCL) cell lines. It has been suggested that their survival does not solely rely on the BCR pathway; thus, they were not successfully targeted by ibrutinib in clinical studies. However, compared with ibrutinib, the antiproliferative potency of compounds **31** and **38** was approximately 13-fold stronger against SU-DHL-6 cells and 35-fold stronger against WSU-NHL cells (Table 6). We are actively investigating the biological basis for these results and will report our findings in due course. One

Table 6. Antiproliferation Activity against Several Cancer Cell Lines^a

compd	GI_{50} (μ M)			
	DoHH2	Pfeiffer	SU-DHL-6	WSU-NHL
ibrutinib	0.41	0.002	0.58	1.09
31	0.073	0.008	0.038	0.031
38	0.040	0.008	0.043	0.029

^a GI_{50} values are reported as mean values of two or three independent experiments in triplicate.

direction is to examine the changes of proteins directly involved in the BCR pathway, and the other one is to investigate potential involvements of additional pathways because of the fact that these compounds are also potent against quite a few of kinases with important functions. Overall, these results are certainly encouraging for potentially expanded applications of Btk inhibitors in clinical studies.

Pharmacokinetic Properties of Compounds **31 and **38**.** Both compounds **31** and **38** displayed fair solubility and excellent stability in fasted state simulated intestinal fluid (FaSSIF) (Table 7),⁶⁶ which mimics the human intestinal environment. We estimated that these compounds would have a moderate hepatic clearance rate in mice based on a mouse microsome stability study. However, in vivo pharmacokinetic studies in mice showed that compound **31** had a fair half-life of 2.8 h, whereas compound **38** had a much shorter half-life of 0.6 h. Both compounds had small distribution volumes, and they were expected to primarily remain in the circulatory system.

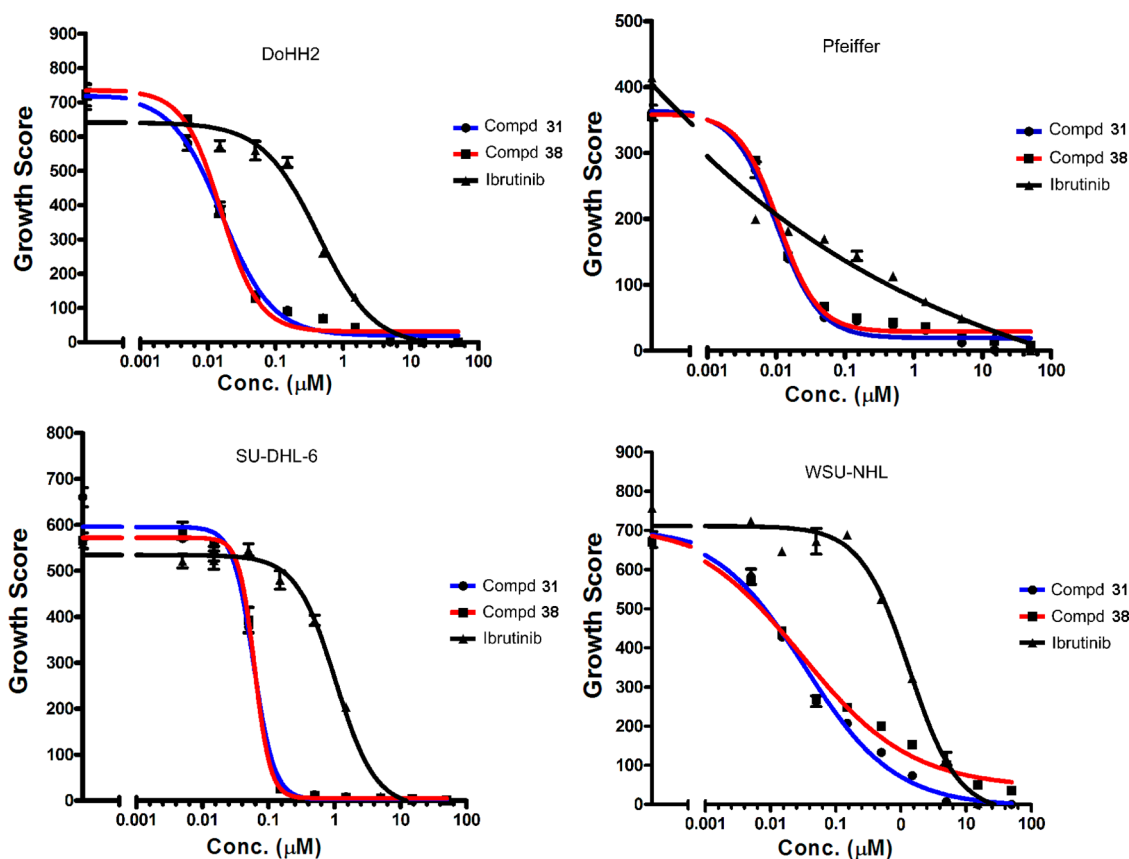


Figure 7. Tumor cell proliferation assays. Representative dose–response curves of **31**, **38**, and ibrutinib treating DoHH2, Pfeiffer, SU-DHL-6, and WSU-NHL cells. Cells were seeded in 96-well plates, incubated for 24 h, then treated with compounds for 72 h, and measured with a luminescent cell viability assay.

Table 7. Select PK Parameters for Compounds 31 and 38

parameter	compound	
	31	38
FaSSiF		
solubility (μM)	7.02	2.23
stability (% remaining at 24 h)	94	99
Mouse Liver Microsome		
$t_{1/2}$ (h)	0.64	0.59
CL ($\mu\text{L min}^{-1} \text{mg}^{-1}$)	25.7	28.1
CL ^{hsp} ($\text{mL min}^{-1} \text{kg}^{-1}$)	47.8	49.8
In Vivo (iv) ^a		
$t_{1/2}$ (h)	2.8	0.6
CL ($\text{mL min}^{-1} \text{kg}^{-1}$)	6.85	11.49
V_{ss} (L/kg)	0.20	0.13

^aThe in vivo pharmacokinetics of compounds 31 and 38 were evaluated in ICR mice ($n = 3$) following intravenous (iv) injection at 1 mg/kg dose level. At various time points, blood samples were collected and analyzed by LC–MS method.

In Vivo Efficacy of Compound 31. On the basis of its potency and PK properties, compound 31 was further examined in a mouse xenograft model inoculated with the human lymphoma DoHH2 cells. This study comprised four groups, with a vehicle control group and three treatment groups that included one dose of ibrutinib (10 mg/kg) and two doses of compound 31 (10 and 20 mg/kg). Ibrutinib was used as a positive control because its in vivo antiproliferative effects in a xenograft model of DoHH2 have been reported in the literature.⁶⁷ The compounds were administered through the tail vein once a day for 14 consecutive days, and the tumor sizes were measured periodically. Plasma concentrations of compounds were determined at 2 and 24 h after the last drug administration. While all treatment groups achieved nice exposure of compounds at 2 h, neither the 10 mg/kg ibrutinib nor the 10 mg/kg compound 31 treatment groups had any detectable levels of compounds at 24 h and the 20 mg/kg compound 31 treatment group showed a dramatically reduced drug concentration (Supporting Information). As shown in Figure 8, at the end of the study, tumor sizes of the ibrutinib-treated group were reduced by 32% ($P = 0.145$), and both compound 31 dosage groups displayed more potent antiproliferative effects. Compared with the vehicle control group, the tumor size was reduced by 60% ($P = 0.016$) in the 10 mg/kg compound 31 treatment group, whereas the tumor size was reduced by 66% ($P = 0.004$) in the 20 mg/kg group. In every group, the mice slightly gained weight after the 14-day treatment, and no significant weight fluctuations were observed during the treatment. Thus, compound 31 was well-tolerated and exhibited a clear antiproliferative effect in this mouse xenograft model.

CHEMISTRY

The syntheses of this novel series of compounds were outlined in Schemes 1, 2, and 3 where the core structure was prepared using a method previously reported by Amgen scientists.⁵⁶ In general, reactions proceeded smoothly and provided desired products in good yields. Compound 42 was coupled with various amines, followed by a reduction step to form intermediates 43, which underwent amide condensation to yield compounds 4–10 (Scheme 1).

As shown in Scheme 2, aniline 44 was prepared from compound 42 via S_NAr reaction followed by catalytic reduction.

Condensation reactions with aromatic acids with variations at the R position, followed by deprotection of the Boc group, afforded compounds 12 and 16–18. 12 was further acylated with different reactive groups or other acids to yield compounds 13–15, 31–38. Compound 11 with an amino group at the para position was prepared in a manner similar to that for 12 (Supporting Information). Reverse amide and urea compounds (19 and 20) were prepared using similar methods based on Amgen's procedures, which were also described in the Supporting Information.

An alternative synthetic route is outlined in Scheme 3. Cbz-protected compound 45 was coupled with 44 followed by removal of the Cbz group to afford intermediate 46. Compounds 21–30 were prepared by amide coupling with various carboxylic acids and the removal of Boc protection group. Finally, compounds 39–41 were obtained by acylating amine precursors with acryloyl chloride.

CONCLUSIONS

We developed novel covalent irreversible inhibitors of Btk based on a type II scaffold. These compounds exhibited potent inhibitory activity in biochemical and cellular assays, presented a dual-action mode of inhibition that counteracted the negative regulation loop for Btk, and have a different selectivity profile from ibrutinib. These inhibitors were up to 35-fold more potent than the leading clinical drug, ibrutinib, in lymphoma cell viability assays. In a mouse xenograft model, compound 31 effectively prevented lymphoma tumor growth in a dose-dependent manner. Because of the emerging importance of Btk in a wide range of B-cell lineage hematological cancers, our results support a new direction for the development of novel Btk inhibitors. Further optimization of this series of compounds will be reported in due course.

EXPERIMENTAL SECTION

Chemistry. All materials were obtained from commercial suppliers and used without further purification unless otherwise noted. Yields refer to chromatographic yields unless otherwise stated. Anhydrous THF was distilled from sodium. DCM and toluene were distilled from calcium hydride. Reactions were monitored by thin-layer chromatography (TLC) carried out on 0.25 mm Yantai silica gel plates (HSGF 254) using UV light as visualizing agents or an ethanolic solution of phosphomolybdic acid or ninhydrin as developing agents. Yantai silica gel (ZCX-II, particle size 0.048–0.075 mm) was used for flash column chromatography. ^1H NMR and ^{13}C NMR spectra were recorded on a Bruker Avance 300 (^1H , 300 MHz; ^{13}C , 75 MHz) or Bruker Avance 400 (^1H , 400 MHz; ^{13}C , 100 MHz) or Bruker Avance 500 (^1H , 500 MHz; ^{13}C , 125 MHz) spectrometer at ambient temperature. Chemical shifts are reported in ppm from the solvent resonance. Data are reported as follows: chemical shift, multiplicity (s = singlet, d = doublet, t = triplet, q = quartet, br = broad, m = multiplet), coupling constants, and number of protons. Mass spectrometric data were obtained using an AB Q-Star mass spectrometer. All final compounds (4–41) were purified to >95% purity as determined by high performance liquid chromatography (HPLC) with UV detection at 254 nm. HPLC experiments were performed on an Agilent 1200 series LC system equipped with a quaternary pump (G1311A), a vacuum degasser (G1322A), a diode array detector (G1315D), and an autosampler (G1329A) using an Agilent Eclipse Plus C18 (5 μm , 4.6 mm \times 250 mm) column. The mobile phase was constituted of H_2O and CH_3CN (eluent A, 30–100% CH_3CN , 15 min; 100% CH_3CN , 5 min; 1.00 mL/min flow rate; eluent B, 30–100% 0.1% TFA in CH_3CN /0.1% TFA in H_2O , 15 min; 100% 0.1% TFA in CH_3CN , 5 min; 1.00 mL/min flow rate).

Synthesis of tert-Butyl 3-(5-Aminopyrimidin-2-ylamino)-phenylcarbamate (44). Step 1. Potassium carbonate (0.702 g,

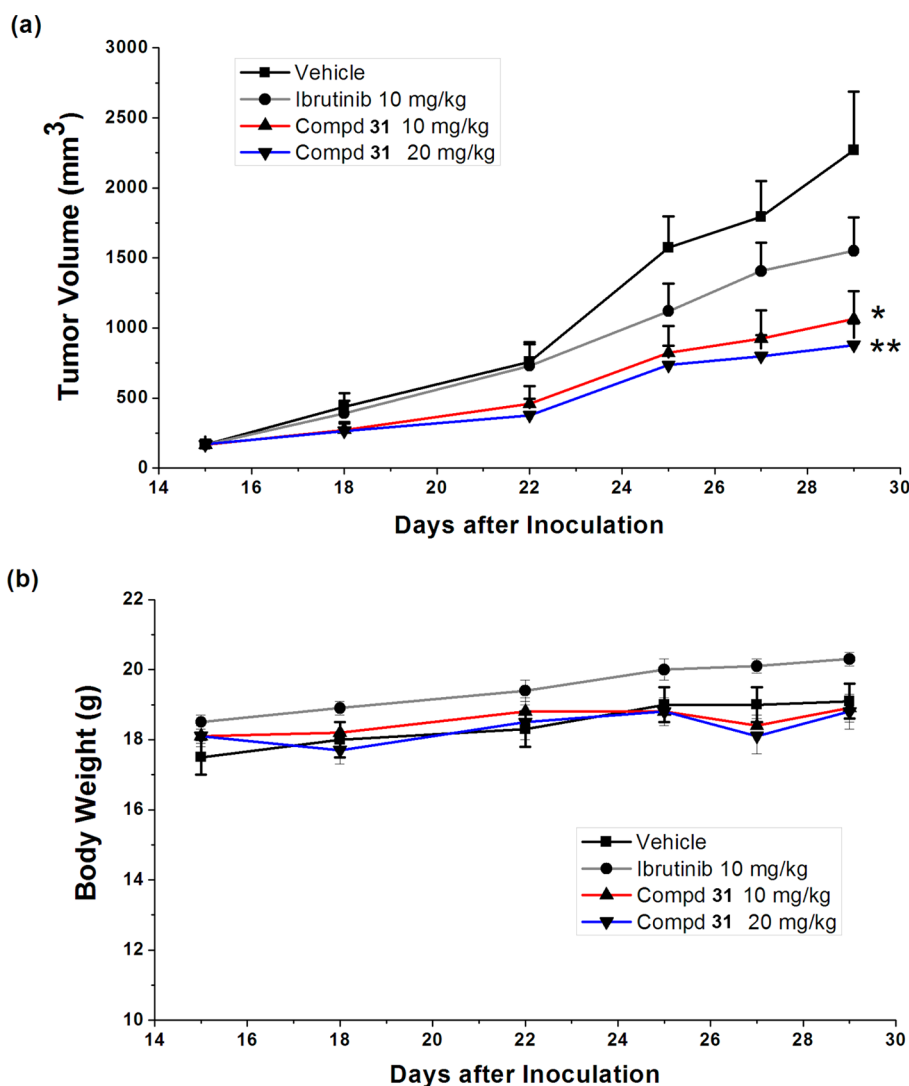
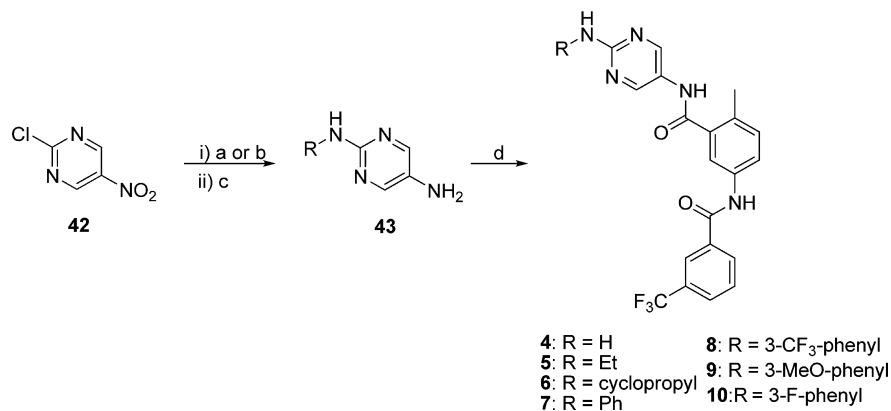
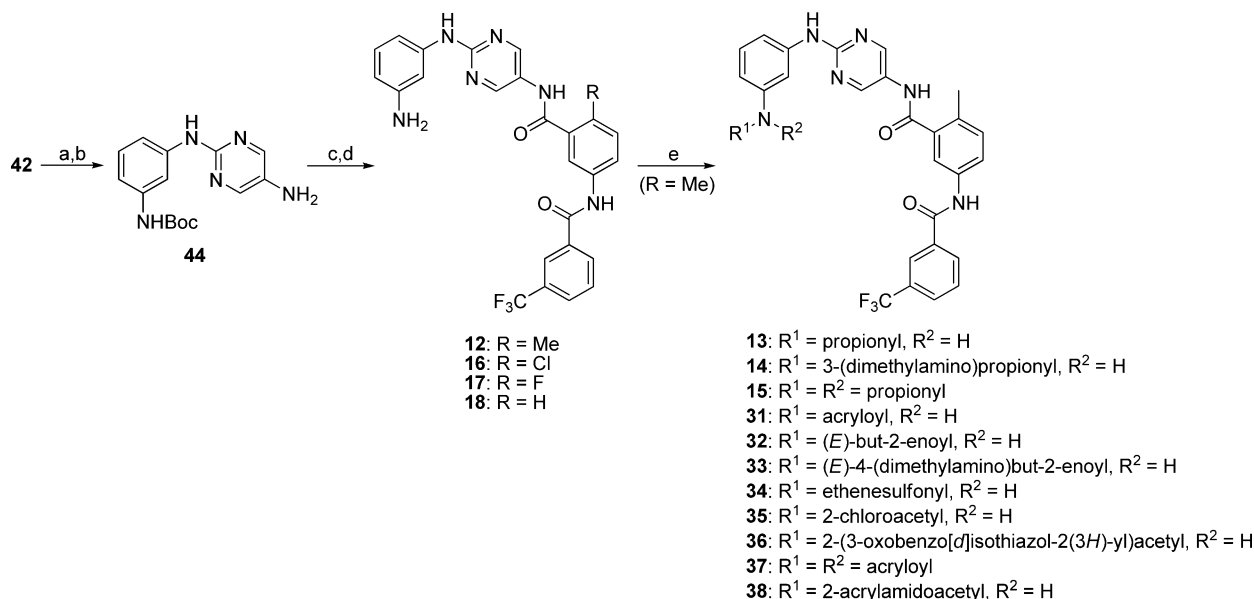


Figure 8. Btk inhibitor 31 in vivo efficacy study. (a) Compound 31 significantly prevented tumor growth in a xenograft mouse model. DoHH2 cells were implanted subcutaneously in female CB17/SCID mice. When tumors reached $\sim 167 \text{ mm}^3$ on average, mice were randomized into four groups ($n = 6/\text{group}$). Compounds were administered via tail vein as a clear solution in polyoxyl 15 hydroxystearate/ethanol (1:1). Tumor size and weight were monitored periodically for 14 days. Statistical analysis was conducted by one-way ANOVA. The Dunnett test was used to analyze the statistical significance between each treatment group and the vehicle group. (*) $P < 0.05$ and (**) $P < 0.01$ indicate statistical significance of tumor growth inhibition. (b) The body weights of the mice changed over time, and the mice in every group slightly gained weight at the end of the study.

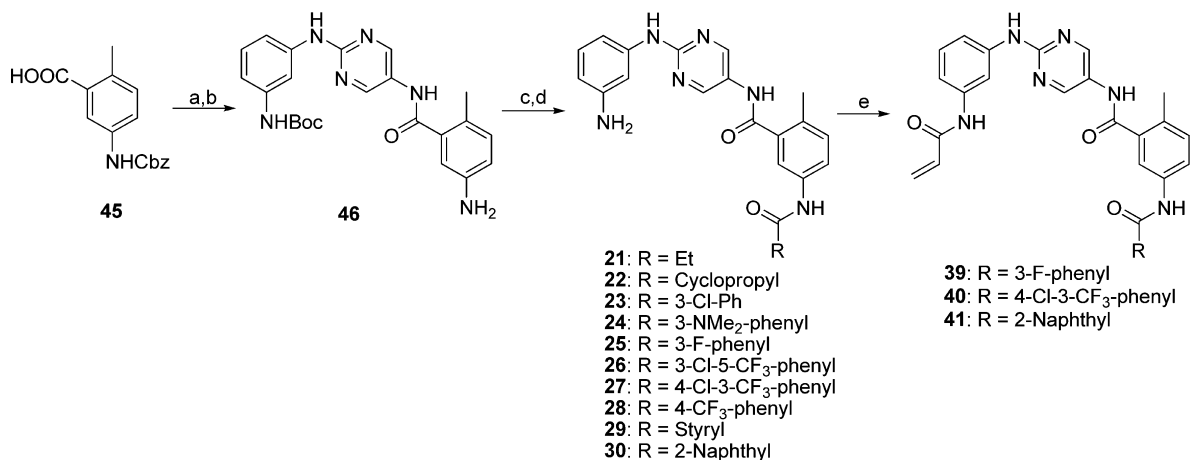
Scheme 1. Preparation of Compounds 4–10^a



^aReagents and conditions: (a) ammonium hydroxide, THF, rt, 1 h (96%); (b) R-NH₂, K₂CO₃, CH₃CN, H₂O, rt, 3 h (81–96%); (c) 5% Pd/C, H₂, methanol, rt, overnight (88–93%); (d) 2-methyl-5-(3-(trifluoromethyl)benzamido)benzoic acid, HATU, DIEA, DMF, rt, 8 h (71–98%).

Scheme 2. Preparation of Compounds 12–18, 31–38^a

^aReagents and conditions: (a) 3-(*tert*-butoxycarbonylamino)aniline or 4-(*tert*-butoxycarbonylamino)aniline, K₂CO₃, CH₃CN, H₂O, rt, 3 h (89%); (b) 5% Pd/C, H₂, methanol, rt, overnight (88%); (c) various aromatic acids, HATU, DIEA, DMF, rt, 6 h (72–80%); (d) TFA, DCM, rt, 2 h (71–98%); (e) various acyl chlorides, THF–H₂O, rt, 1 h (13, 91%; 31, 90%; 35, 87%); or various carboxylic acids, HATU, DIEA, DMF, rt, 5 h (14, 73%; 32, 90%; 33, 83%; 36, 81%; 38, 88%); or various acyl chlorides, THF, rt, 1 h (15, 91%; 37, 93%); or 2-chloroethanesulfonyl chloride, DIEA, DMAP, THF, rt, 7 h (34, 84%).

Scheme 3. Alternative Route to 2,5-Diaminopyrimidines 21–30, 39–41^a

^aReagents and conditions: (a) 44, HATU, DIEA, DMF, 5 h (71%); (b) 5% Pd/C, H₂, methanol, 60 °C, 10 h (53%); (c) R-COOH, HATU, DMF, rt, 5 h (82–93%); (d) TFA, DCM, rt, 3 h (88–91%); (e) acryloyl chloride, THF, H₂O, rt, 1 h (84–98%).

5.08 mmol) was added to a stirred solution of 2-chloro-5-nitropyrimidine (42) (0.352 g, 1.69 mmol) and *tert*-butyl 3-aminophenylcarbamate (0.270 g, 1.69 mmol) in acetonitrile (12 mL), and the mixture was stirred for 3 h at room temperature. The solution was diluted with water and extracted twice with ethyl acetate. The combined organic layers were dried, concentrated under vacuum, and purified via column chromatography (gradient, 20–75% EtOAc in hexanes) to yield *tert*-butyl 3-(5-nitropyrimidin-2-ylamino)phenylcarbamate (0.500 g, 89%) as yellow solids.

Step 2. *tert*-Butyl 3-(5-nitropyrimidin-2-ylamino)phenylcarbamate (0.500 g, 1.51 mmol) and 5% Pd/C (0.16 g) were dissolved in 10 mL of methanol, and then the mixture was stirred under hydrogen atmosphere at room temperature for 5 h. Once the reaction was completed, the mixture was filtered through Celite and the filtrate was concentrated and purified by column chromatography (gradient, 50–85% EtOAc in hexanes) to give the title compound (0.40 g, 88%)

as yellow solids. ¹H NMR (400 MHz, DMSO-*d*₆): δ 9.13 (s, 1H), 8.86 (s, 1H), 7.95 (s, 2H), 7.77 (s, 1H), 7.25 (d, 1H, *J* = 8.1 Hz), 7.05 (t, 1H, *J* = 8.1 Hz), 6.92 (d, 1H, *J* = 7.8 Hz), 4.77 (s, 2H), 1.47 (s, 9H). ¹³C NMR (125 MHz, DMSO-*d*₆): δ 152.8, 152.7, 143.6, 141.9, 139.4, 135.5, 128.0, 111.7, 110.5, 107.9, 78.5, 28.0. HRMS (ESI) *m/z* calculated for C₁₅H₂₀N₅O₂⁺ [*M* + *H*]⁺: 302.1617. Found: 302.1602.

Synthesis of *N*-(2-(3-Aminophenylamino)pyrimidin-5-yl)-2-methyl-5-(3-(trifluoromethyl)benzamido)benzamide (12). **Step 1.** 44 (0.100 g, 0.230 mmol), 3-(trifluoromethyl)benzoic acid (0.048 g, 0.25 mmol), and HATU (0.131 g, 0.345 mmol) were dissolved in DMF (2 mL), followed by the addition of DIEA (0.075 mL, 0.46 mmol). The mixture was stirred at room temperature for 7 h. Then the solution was concentrated under vacuum and the residue was diluted with saturated aqueous sodium bicarbonate and ethyl acetate. The aqueous phase was separated and extracted twice with ethyl acetate. The combined organic phases were washed with brine, dried over anhydrous magnesium

sulfate, concentrated, and purified by column chromatography (gradient, 30–100% EtOAc in hexanes) to yield *tert*-butyl 3-(5-(2-methyl-5-(3-(trifluoromethyl)benzamido)benzamido)pyrimidin-2-ylamino)-phenylcarbamate (0.12 g) as yellow solids.

Step 2. 3-(5-(2-Methyl-5-(3-(trifluoromethyl)benzamido)-benzamido)pyrimidin-2-ylamino)phenylcarbamate (0.120 g, 0.198 mmol) was treated with TFA (2 mL) and DCM (2 mL). The mixture was stirred at room temperature for 2 h and concentrated under vacuum. The residue was diluted with saturated aqueous sodium bicarbonate and ethyl acetate. The organic phase was separated and washed with brine, dried over anhydrous magnesium sulfate, concentrated, and purified by column chromatography (gradient, 50–80% EtOAc in hexanes) to give the title compound (0.096 g, 82% for two steps) as white solids. ^1H NMR (500 MHz, $\text{DMSO}-d_6$): δ 10.56 (s, 1H), 10.36 (s, 1H), 9.30 (s, 1H), 8.76 (s, 2H), 8.33 (s, 1H), 8.28 (d, 1H, $J = 7.9$ Hz), 7.98 (d, 1H, $J = 7.8$ Hz), 7.93 (d, 1H, $J = 2.0$ Hz), 7.85 (dd, 1H, $J = 2.0$ Hz, $J = 8.3$ Hz), 7.80 (t, 1H, $J = 7.9$ Hz), 7.33 (d, 1H, $J = 8.4$ Hz), 7.07 (s, 1H), 6.89 (t, 1H, $J = 7.8$ Hz), 6.84 (d, 1H, $J = 8.1$ Hz), 6.17 (d, 1H, $J = 7.6$ Hz), 4.94 (s, 2H), 2.39 (s, 3H). ^{13}C NMR (100 MHz, $\text{DMSO}-d_6$): δ 167.5, 163.9, 156.8, 149.8, 148.8, 141.1, 136.5, 136.4, 135.5, 131.8, 130.9, 130.8, 129.8, 129.3, 129.0, 128.6, 128.2, 125.8, 124.1, 121.7, 119.2, 107.7, 107.0, 104.2, 18.8. HRMS (ESI) m/z calculated for $\text{C}_{26}\text{H}_{20}\text{F}_3\text{N}_6\text{O}_2^-$ [$\text{M} - \text{H}$] $^-$: 505.1600. Found: 505.1591.

Synthesis of *N*-(2-(3-Acrylamidophenylamino)pyrimidin-5-yl)-2-methyl-5-(3-(trifluoromethyl)benzamido)benzamide (31). To a stirred suspension of **12** (0.080 g, 0.16 mmol) and DIEA (0.027 mL, 0.16 mmol) in 1 mL of THF and 1 mL of H_2O was added acryloyl chloride (0.013 mL, 0.16 mmol). Then the mixture was kept stirring at room temperature for 1 h, then concentrated and diluted with ethyl acetate and 10% aqueous citric acid. The organic phase was separated, washed with brine, dried over anhydrous magnesium sulfate, and purified by column chromatography (gradient, 50–70% EtOAc in hexanes) to yield the title compound (0.080 g, 90%) as a white powder. ^1H NMR (300 MHz, $\text{DMSO}-d_6$): δ 10.59 (s, 1H), 10.44 (s, 1H), 10.10 (s, 1H), 9.69 (s, 1H), 8.82 (s, 2H), 8.33 (s, 1H), 8.28 (d, 1H, $J = 8.0$ Hz), 8.07 (s, 1H), 7.99 (d, 1H, $J = 7.8$ Hz), 7.94 (d, 1H, 2.0 Hz), 7.87–7.78 (m, 2H), 7.39–7.32 (m, 3H), 7.23–7.17 (m, 1H), 6.48 (dd, 1H, $J = 10.0$ Hz, $J = 17.0$ Hz), 6.25 (dd, 1H, $J = 2.0$ Hz, $J = 17.0$ Hz), 5.73 (dd, 1H, $J = 1.9$ Hz, $J = 10.0$ Hz), 2.39 (s, 3H). ^{13}C NMR (100 MHz, MeOD): δ 177.0, 173.4, 172.5, 166.0, 159.3, 150.4, 148.6, 146.0, 145.0, 141.5, 141.3, 140.4, 140.3, 139.3, 138.8, 138.5, 138.1, 137.7, 136.0, 135.8, 134.8, 133.6, 131.2, 128.7, 123.5, 122.2, 119.0, 28.3. HRMS (ESI) m/z calculated for $\text{C}_{29}\text{H}_{24}\text{F}_3\text{N}_6\text{O}_3^+$ [$\text{M} + \text{H}$] $^+$: 561.1862. Found: 561.1859.

***N*-(2-Aminopyrimidin-5-yl)-2-methyl-5-(3-(trifluoromethyl)benzamido)benzamide (4).** White solids. ^1H NMR (300 MHz, $\text{DMSO}-d_6$): δ 10.57 (s, 1H), 10.17 (s, 1H), 8.51 (s, 2H), 8.32 (s, 1H), 8.27 (d, 1H, $J = 7.7$ Hz), 7.98 (d, 1H, $J = 8.4$ Hz), 7.89 (d, 1H, $J = 2.2$ Hz), 7.84–7.77 (m, 2H), 7.30 (d, 1H, $J = 8.4$ Hz), 6.55 (s, 2H), 2.36 (s, 3H). ^{13}C NMR (125 MHz, $\text{DMSO}-d_6$): δ 167.3, 163.8, 160.5, 150.7, 136.7, 136.3, 135.4, 131.6, 130.7, 130.6, 129.6, 128.04, 128.01, 124.2, 124.0, 123.9, 121.5, 119.1, 18.6. HRMS (ESI) m/z calculated for $\text{C}_{20}\text{H}_{17}\text{F}_3\text{N}_5\text{O}_2^+$ [$\text{M} + \text{H}$] $^+$: 416.1334. Found: 416.1338.

***N*-(2-(Ethylamino)pyrimidin-5-yl)-2-methyl-5-(3-(trifluoromethyl)benzamido)benzamide (5).** White solids. ^1H NMR (400 MHz, $\text{DMSO}-d_6$): δ 10.56 (s, 1H), 10.15 (s, 1H), 8.55 (s, 1H), 8.32 (s, 1H), 8.28 (d, 1H, $J = 7.9$ Hz), 7.98 (d, 1H, $J = 7.8$ Hz), 7.89 (d, 1H, $J = 2.2$ Hz), 7.85–7.78 (m, 2H), 7.30 (d, 1H, $J = 8.4$ Hz), 7.07 (t, 1H, $J = 5.6$ Hz), 3.30–3.26 (m, 2H), 2.37 (s, 3H), 1.12 (t, 3H, $J = 7.1$ Hz). ^{13}C NMR (100 MHz, $\text{DMSO}-d_6$): δ 168.9, 165.4, 160.9, 152.3, 138.2, 137.9, 137.0, 133.3, 132.7, 132.4, 132.2, 131.3, 130.8, 129.7, 125.6, 125.4, 123.1, 120.7, 37.1, 20.3, 16.2. HRMS (ESI) m/z calculated for $\text{C}_{22}\text{H}_{19}\text{F}_3\text{N}_5\text{O}_2^-$ [$\text{M} - \text{H}$] $^-$: 442.1491. Found: 442.1496.

***N*-(2-(Cyclopropylamino)pyrimidin-5-yl)-2-methyl-5-(3-(trifluoromethyl)benzamido)benzamide (6).** White solids. ^1H NMR (500 MHz, $\text{DMSO}-d_6$): δ 10.55 (s, 1H), 10.17 (s, 1H), 8.58 (s, 1H), 8.32–8.27 (m, 3H), 7.97 (d, 1H, $J = 7.6$ Hz), 7.89 (d, 1H, $J = 2.0$ Hz), 7.84–7.78 (m, 2H), 7.32–7.29 (m, 2H), 2.68–2.66 (m, 1H), 2.36 (s, 3H), 0.67–0.63 (m, 2H), 0.47–0.43 (m, 2H). ^{13}C NMR (100 MHz, $\text{DMSO}-d_6$): δ 167.4, 163.9, 160.3, 150.6, 136.7, 136.4,

135.4, 131.8, 130.8, 130.7, 129.8, 128.2, 124.5, 124.1, 123.6, 122.2, 121.6, 119.2, 23.9, 18.8, 6.4. HRMS (ESI) m/z calculated for $\text{C}_{23}\text{H}_{21}\text{F}_3\text{N}_5\text{O}_2^+$ [$\text{M} + \text{H}$] $^+$: 456.1647. Found: 456.1642.

2-Methyl-*N*-(2-(phenylamino)pyrimidin-5-yl)-5-(3-(trifluoromethyl)benzamido)benzamide (7). White solids. ^1H NMR (400 MHz, $\text{DMSO}-d_6$): δ 10.57 (s, 1H), 10.41 (s, 1H), 9.63 (s, 1H), 8.80 (s, 2H), 8.33 (s, 1H), 8.28 (d, 1H, $J = 8.0$ Hz), 7.98 (d, 1H, $J = 7.6$ Hz), 7.93 (d, 1H, $J = 2.0$ Hz), 7.84 (dd, 1H, $J = 2.1$ Hz, $J = 8.3$ Hz), 7.80 (t, 1H, $J = 7.8$ Hz), 7.74 (d, 2H, $J = 7.8$ Hz), 7.33 (d, 1H, $J = 8.4$ Hz), 7.27 (t, 2H, $J = 8.1$ Hz), 6.93 (t, 1H, $J = 7.3$ Hz), 2.39 (s, 3H). ^{13}C NMR (100 MHz, $\text{DMSO}-d_6$): δ 167.5, 163.9, 156.5, 149.9, 140.6, 136.5, 135.4, 131.8, 130.9, 130.8, 129.8, 129.3, 129.0, 128.4, 128.2, 126.2, 124.1, 121.7, 121.0, 119.2, 118.4, 118.3, 18.8. HRMS (ESI) m/z calculated for $\text{C}_{26}\text{H}_{21}\text{F}_3\text{N}_5\text{O}_2^+$ [$\text{M} + \text{H}$] $^+$: 492.1647. Found: 492.1650.

2-Methyl-5-(3-(trifluoromethyl)benzamido)-*N*-(2-(3-(trifluoromethyl)phenylamino)pyrimidin-5-yl)benzamide (8). White solids. ^1H NMR (400 MHz, $\text{DMSO}-d_6$): δ 10.59 (s, 1H), 10.50 (s, 1H), 10.03 (s, 1H), 8.87 (s, 2H), 8.33 (s, 1H), 8.28 (d, 1H, $J = 7.9$ Hz), 8.22 (s, 1H), 7.99 (t, 2H, $J = 9.6$ Hz), 7.94 (d, 1H, $J = 2.2$ Hz), 7.86–7.78 (m, 2H), 7.51 (t, 1H, $J = 8.0$ Hz), 7.33 (d, 1H, $J = 8.5$ Hz), 7.25 (d, 1H, $J = 7.7$ Hz), 2.39 (s, 3H). ^{13}C NMR (100 MHz, $\text{DMSO}-d_6$): δ 169.5, 165.8, 158.0, 151.7, 143.3, 138.4, 138.3, 137.3, 133.7, 132.9, 132.8, 131.7, 131.5, 130.2, 128.8, 127.6, 127.2, 126.0, 124.9, 124.5, 123.7, 123.5, 121.5, 118.9, 115.7, 20.7. HRMS (ESI) m/z calculated for $\text{C}_{27}\text{H}_{18}\text{F}_6\text{N}_5\text{O}_2^-$ [$\text{M} - \text{H}$] $^-$: 558.1365. Found: 558.1370.

***N*-(2-(3-Methoxyphenylamino)pyrimidin-5-yl)-2-methyl-5-(3-(trifluoromethyl)benzamido)benzamide (9).** White solids. ^1H NMR (400 MHz, $\text{DMSO}-d_6$): δ 10.59 (s, 1H), 10.44 (s, 1H), 9.63 (s, 1H), 8.81 (d, 2H, $J = 2.2$ Hz), 8.32 (s, 1H), 8.28 (d, 1H, $J = 7.8$ Hz), 7.98 (d, 1H, $J = 7.4$ Hz), 7.94 (s, 1H), 7.85–7.78 (m, 2H), 7.48 (d, 1H, $J = 1.8$ Hz), 7.32 (t, 2H, $J = 8.8$ Hz), 7.19–7.14 (m, 1H), 6.50 (d, 1H, $J = 8.0$ Hz), 3.73 (d, 3H, $J = 2.2$ Hz), 2.38 (s, 3H). ^{13}C NMR (125 MHz, $\text{DMSO}-d_6$): δ 167.5, 163.8, 159.5, 156.4, 149.8, 141.7, 136.4, 135.4, 131.6, 130.8, 130.7, 129.6, 129.0, 128.1, 126.2, 124.0, 121.7, 119.2, 110.8, 106.2, 104.3, 54.8, 18.6. HRMS (ESI) m/z calculated for $\text{C}_{27}\text{H}_{21}\text{F}_3\text{N}_5\text{O}_3^-$ [$\text{M} - \text{H}$] $^-$: 520.1596. Found: 520.1600.

***N*-(2-(3-Fluorophenylamino)pyrimidin-5-yl)-2-methyl-5-(3-(trifluoromethyl)benzamido)benzamide (10).** White solids. ^1H NMR (400 MHz, $\text{DMSO}-d_6$): δ 10.59 (s, 1H), 10.49 (s, 1H), 9.92 (s, 1H), 8.86 (s, 2H), 8.33 (s, 1H), 8.28 (d, 1H, $J = 7.8$ Hz), 7.98 (d, 1H, $J = 7.5$ Hz), 7.95 (s, 1H), 7.86–7.78 (m, 3H), 7.47 (d, 1H, $J = 8.0$ Hz), 7.35–7.26 (m, 2H), 6.72 (td, 1H, $J = 2.1$ Hz, $J = 8.4$ Hz), 2.39 (s, 3H). ^{13}C NMR (100 MHz, $\text{DMSO}-d_6$): δ 169.5, 165.8, 165.4, 163.1, 158.0, 151.7, 144.3, 138.4, 137.3, 133.7, 132.9, 131.9, 131.7, 131.2, 130.1, 128.7, 127.2, 126.0, 124.5, 123.7, 121.1, 115.9, 109.1, 106.5, 20.7. HRMS (ESI) m/z calculated for $\text{C}_{26}\text{H}_{18}\text{F}_4\text{N}_5\text{O}_2^-$ [$\text{M} - \text{H}$] $^-$: 508.1397. Found: 508.1402.

***N*-(2-(4-Aminophenylamino)pyrimidin-5-yl)-2-methyl-5-(3-(trifluoromethyl)benzamido)benzamide (11).** White solids. ^1H NMR (300 MHz, MeOD): δ 8.64 (s, 2H), 8.27 (s, 1H), 8.20 (d, 1H, $J = 8.1$ Hz), 7.93–7.88 (m, 2H), 7.74 (d, 1H, $J = 7.9$ Hz), 7.67 (dd, 1H, $J = 2.2$ Hz, $J = 8.2$ Hz), 7.34–7.31 (m, 3H), 6.74 (d, 2H, $J = 8.7$ Hz), 4.63 (s, 3H), 2.45 (s, 2H). ^{13}C NMR (100 MHz, $\text{DMSO}-d_6$): δ 167.4, 163.9, 157.5, 157.3, 151.3, 150.2, 143.6, 143.4, 136.6, 136.4, 135.4, 134.9, 131.8, 130.9, 129.8, 128.2, 125.0, 124.1, 121.1, 120.9, 119.2, 114.0, 18.8. HRMS (ESI) m/z calculated for $\text{C}_{26}\text{H}_{22}\text{F}_3\text{N}_6\text{O}_2^+$ [$\text{M} + \text{H}$] $^+$: 507.1756. Found: 507.1741.

2-Methyl-*N*-(2-(3-propionamidophenylamino)pyrimidin-5-yl)-5-(3-(trifluoromethyl)benzamido)benzamide (13). White solids. ^1H NMR (300 MHz, $\text{DMSO}-d_6$): δ 10.59 (s, 1H), 10.43 (s, 1H), 9.81 (s, 1H), 9.63 (s, 1H), 8.80 (s, 2H), 8.32 (s, 1H), 8.28 (d, 1H, $J = 7.8$ Hz), 7.98–7.93 (m, 3H), 7.86–7.77 (m, 2H), 7.33 (d, 2H, $J = 8.3$ Hz), 7.28 (d, 1H, $J = 7.7$ Hz), 7.15 (t, 1H, $J = 8.1$ Hz), 2.38 (s, 3H), 2.30 (q, 2H, $J = 7.5$ Hz), 1.07 (t, 3H, $J = 7.5$ Hz). ^{13}C NMR (100 MHz, $\text{DMSO}-d_6$): δ 173.7, 169.4, 165.8, 158.5, 151.7, 142.7, 141.4, 138.4, 138.3, 137.4, 133.7, 132.9, 132.7, 131.7, 131.2, 130.9, 130.3, 130.1, 128.2, 126.0, 123.7, 121.1, 115.5, 114.4, 111.3, 31.3, 20.7, 11.6. HRMS (ESI) m/z calculated for $\text{C}_{29}\text{H}_{26}\text{F}_3\text{N}_6\text{O}_3^+$ [$\text{M} + \text{H}$] $^+$: 563.2018. Found: 563.2012.

N-(2-(3-(3-(Dimethylamino)propanamido)phenylamino)pyrimidin-5-yl)-2-methyl-5-(3-(trifluoromethyl)benzamido)benzamide (14). White solids. ^1H NMR (400 MHz, DMSO- d_6): δ 10.59 (s, 1H), 10.43 (s, 1H), 10.13 (s, 1H), 9.67 (s, 1H), 8.81 (s, 2H), 8.32 (s, 1H), 8.28 (d, 1H, J = 7.9 Hz), 8.03 (s, 1H), 7.99–7.96 (m, 2H), 7.84–7.78 (m, 2H), 7.36–7.28 (m, 3H), 7.21–7.17 (m, 1H), 3.28–3.06 (m, 4H), 2.94–2.90 (m, 1H), 2.79 (t, 1H, J = 7.0 Hz), 2.74 (s, 4H), 2.39 (s, 3H). ^{13}C NMR (100 MHz, DMSO- d_6): δ 168.0, 167.5, 163.9, 156.4, 149.8, 140.9, 139.0, 136.5, 136.4, 135.4, 131.8, 130.9, 130.8, 129.8, 128.6, 128.2, 126.3, 125.3, 124.1, 122.6, 121.8, 119.3, 113.9, 112.4, 109.4, 52.9, 42.6, 31.2, 18.8. HRMS (ESI) m/z calculated for $\text{C}_{31}\text{H}_{31}\text{F}_3\text{N}_7\text{O}_3$ $[\text{M} + \text{H}]^+$: 606.2440. Found: 606.2433.

2-Methyl-N-(2-(3-(N-propionylpropionamido)phenylamino)pyrimidin-5-yl)-5-(3-(trifluoromethyl)benzamido)benzamide (15). White solids. ^1H NMR (500 MHz, DMSO- d_6): δ 10.88 (s, 1H), 10.59 (s, 1H), 9.93 (s, 1H), 9.11 (s, 2H), 8.31 (s, 1H), 8.27 (d, 1H, J = 7.8 Hz), 7.98–7.97 (m, 2H), 7.83 (dd, 1H, J = 2.1 Hz, J = 8.3 Hz), 7.78 (d, 1H, J = 7.8 Hz), 7.53 (1H), 7.49 (d, 1H, J = 8.2 Hz), 7.34 (d, 1H, J = 8.4 Hz), 7.30 (t, 1H, J = 8.0 Hz), 6.89 (d, 1H, J = 8.8 Hz), 2.44 (q, 2H, J = 7.4 Hz), 2.38 (s, 3H), 2.29 (q, 2H, J = 7.6 Hz), 1.07–1.04 (m, 6H). ^{13}C NMR (100 MHz, DMSO- d_6): δ 173.7, 172.1, 168.1, 164.0, 155.9, 149.3, 141.5, 140.0, 136.5, 135.8, 135.4, 132.0, 131.8, 131.1, 131.0, 129.8, 129.1, 128.2, 124.1, 122.2, 119.3, 118.1, 117.4, 29.5, 28.5, 18.8, 9.5, 9.4. HRMS (ESI) m/z calculated for $\text{C}_{32}\text{H}_{30}\text{F}_3\text{N}_6\text{O}_4$ $[\text{M} + \text{H}]^+$: 619.2281. Found: 619.2274.

N-(2-(3-Aminophenylamino)pyrimidin-5-yl)-2-chloro-5-(3-(trifluoromethyl)benzamido)benzamide (16). White solids. ^1H NMR (400 MHz, DMSO- d_6): δ 10.74 (s, 1H), 10.62 (s, 1H), 9.38 (s, 1H), 8.76 (s, 2H), 8.34 (s, 1H), 8.29 (d, 1H, J = 7.9 Hz), 8.06 (d, 1H, J = 2.4 Hz), 8.00 (d, 1H, J = 7.7 Hz), 7.97 (dd, 1H, J = 2.5 Hz, J = 8.8 Hz), 7.82 (t, 1H, J = 7.6 Hz), 7.61 (d, 1H, J = 8.8 Hz), 7.09 (s, 1H), 6.91 (t, 1H, J = 7.7 Hz), 6.86 (d, 1H, J = 8.1 Hz), 6.20 (d, 1H, J = 7.5 Hz), 5.08 (s, 2H). ^{13}C NMR (125 MHz, DMSO- d_6): δ 164.5, 164.1, 156.9, 150.9, 149.7, 148.6, 140.9, 137.8, 136.2, 135.1, 131.7, 131.6, 130.0, 129.7, 128.5, 128.3, 125.4, 124.3, 124.1, 122.8, 120.4, 107.8, 107.1, 104.4. HRMS (ESI) m/z calculated for $\text{C}_{25}\text{H}_{19}\text{ClF}_3\text{N}_6\text{O}_2$ $[\text{M} + \text{H}]^+$: 527.1210. Found: 527.1209.

N-(2-(3-Aminophenylamino)pyrimidin-5-yl)-2-fluoro-5-(3-(trifluoromethyl)benzamido)benzamide (17). White solids. ^1H NMR (500 MHz, MeOD): δ 8.70 (s, 2H), 8.27 (s, 1H), 8.20 (d, 1H, J = 7.9 Hz), 8.13 (dd, 1H, J = 2.7 Hz, J = 6.3 Hz), 7.94–7.91 (m, 1H), 7.88 (d, 1H, J = 7.8 Hz), 7.72 (t, 1H, J = 7.9 Hz), 7.27 (t, 1H, J = 9.3 Hz), 7.20 (t, 1H, J = 2.0 Hz), 7.02 (t, 1H, J = 7.9 Hz), 6.92 (dd, 1H, J = 1.0 Hz, J = 8.1 Hz), 6.40 (dd, 1H, J = 1.3 Hz, J = 7.8 Hz), 4.56 (s, 1H). ^{13}C NMR (125 MHz, MeOD): δ 167.1, 165.0, 164.9, 159.0, 158.9, 156.5, 152.4, 149.1, 142.1, 136.8, 136.4, 136.3, 132.4, 130.7, 130.3, 129.5, 127.1, 126.5, 125.6, 124.4, 123.9, 117.8, 110.9, 107.8. HRMS (ESI) m/z calculated for $\text{C}_{25}\text{H}_{17}\text{F}_4\text{N}_6\text{O}_2$ $[\text{M} - \text{H}]^-$: 509.1349. Found: 509.1355.

N-(2-(3-Aminophenylamino)pyrimidin-5-yl)-3-(3-(trifluoromethyl)benzamido)benzamide (18). White solids. ^1H NMR (400 MHz, DMSO- d_6): δ 10.70 (s, 1H), 10.36 (s, 1H), 9.32 (s, 1H), 8.78 (s, 2H), 8.36 (s, 2H), 8.31 (d, 1H, J = 8.0 Hz), 8.06 (d, 1H, J = 8.2 Hz), 8.00 (d, 1H, J = 7.8 Hz), 7.82 (t, 1H, J = 7.8 Hz), 7.77 (d, 1H, J = 7.9 Hz), 7.57 (t, 1H, J = 7.8 Hz), 7.09 (s, 1H), 6.91 (t, 1H, J = 7.7 Hz), 6.86 (d, 1H, J = 8.0 Hz), 6.19 (d, 1H, J = 7.5 Hz), 4.98 (s, 2H). ^{13}C NMR (125 MHz, DMSO- d_6): δ 165.2, 164.0, 156.8, 150.7, 148.6, 141.0, 138.9, 135.4, 134.7, 131.7, 129.6, 129.0, 128.6, 128.5, 128.1, 125.6, 124.9, 124.1, 123.6, 122.7, 120.0, 107.7, 107.1, 104.3. HRMS (ESI) m/z calculated for $\text{C}_{25}\text{H}_{20}\text{F}_3\text{N}_6\text{O}_2$ $[\text{M} + \text{H}]^+$: 493.1600. Found: 493.1648.

N³-(2-(3-Aminophenylamino)pyrimidin-5-yl)-4-methyl-N¹-(3-(trifluoromethyl)phenyl)isophthalamide (19). White solids. ^1H NMR (300 MHz, MeOD): δ 8.73 (s, 2H), 8.18 (s, 1H), 8.15 (d, 1H, J = 1.8 Hz), 8.00 (dd, 1H, J = 1.9 Hz, J = 8.0 Hz), 7.94 (d, 1H, J = 8.4 Hz), 7.58–7.42 (m, 3H), 7.21 (t, 1H, J = 2.0 Hz), 7.06–6.92 (m, 2H), 6.40 (dt, 1H, J = 1.1 Hz, J = 7.8 Hz), 2.56 (s, 3H). ^{13}C NMR (75 MHz, MeOD): δ 168.8, 166.3, 157.4, 150.7, 147.6, 140.8, 140.6, 139.4, 136.2, 132.0, 131.0, 130.9, 130.5, 129.3, 129.0, 128.8, 126.3, 125.4, 123.7, 120.4, 117.0, 109.7, 109.5, 106.4, 18.5. HRMS (ESI) m/z calculated for $\text{C}_{26}\text{H}_{22}\text{F}_3\text{N}_6\text{O}_2$ $[\text{M} + \text{H}]^+$: 507.1756. Found: 507.1743.

N-(2-(3-Aminophenylamino)pyrimidin-5-yl)-2-methyl-5-(3-(trifluoromethyl)phenyl)ureido)benzamide (20). White solids. ^1H NMR (500 MHz, DMSO- d_6): δ 10.31 (s, 1H), 9.29 (s, 1H), 9.10 (s, 1H), 8.90 (s, 1H), 8.75 (s, 2H), 8.03 (s, 1H), 7.65 (s, 1H), 7.57 (d, 1H, J = 8.0 Hz), 7.51 (t, 1H, J = 7.9 Hz), 7.45 (d, 1H, J = 8.4 Hz), 7.31 (d, 1H, J = 7.4 Hz), 7.23 (d, 1H, J = 8.2 Hz), 7.07 (s, 1H), 6.89 (t, 1H, J = 7.8 Hz), 6.84 (d, 1H, J = 8.0 Hz), 6.17 (d, 1H, J = 7.5 Hz), 4.96 (br s, 2H), 2.34 (s, 3H). ^{13}C NMR (125 MHz, DMSO- d_6): δ 167.5, 156.7, 152.4, 149.8, 148.2, 141.1, 140.4, 136.9, 136.6, 130.8, 129.7, 129.3, 128.7, 128.5, 125.8, 125.2, 121.8, 119.8, 118.0, 117.2, 114.1, 107.8, 107.3, 104.5, 18.5. HRMS (ESI) m/z calculated for $\text{C}_{26}\text{H}_{23}\text{F}_3\text{N}_7\text{O}_2$ $[\text{M} + \text{H}]^+$: 522.1865. Found: 522.1852.

N-(2-(3-Aminophenylamino)pyrimidin-5-yl)-2-methyl-5-propionamidobenzamide (21). White solids. ^1H NMR (500 MHz, DMSO- d_6): δ 10.29 (s, 1H), 9.95 (s, 1H), 9.26 (s, 1H), 8.74 (s, 2H), 7.76 (d, 1H, J = 1.6 Hz), 7.59 (dd, 1H, J = 1.8 Hz, J = 8.2 Hz), 7.22 (d, 1H, J = 8.4 Hz), 7.07 (s, 1H), 6.89 (t, 1H, J = 7.8 Hz), 6.84 (d, 1H, J = 8.2 Hz), 6.18 (d, 1H, J = 1.9 Hz), 4.92 (s, 2H), 2.35–2.30 (m, 5H), 1.09 (t, 3H, J = 7.6 Hz). ^{13}C NMR (125 MHz, DMSO- d_6): δ 172.0, 167.6, 156.7, 149.8, 148.6, 141.0, 136.9, 136.4, 130.7, 129.5, 128.5, 125.8, 120.3, 117.8, 107.7, 107.1, 104.3, 29.4, 18.5, 9.5. HRMS (ESI) m/z calculated for $\text{C}_{21}\text{H}_{23}\text{N}_6\text{O}_2$ $[\text{M} + \text{H}]^+$: 391.1882. Found: 391.1913.

N-(2-(3-Aminophenylamino)pyrimidin-5-yl)-5-(cyclopropanecarboxamido)-2-methylbenzamide (22). White solids. ^1H NMR (400 MHz, DMSO- d_6): δ 10.32 (d, 2H, J = 5.4 Hz), 9.33 (s, 1H), 8.76 (s, 2H), 7.78 (s, 1H), 7.60 (d, 1H, J = 8.2 Hz), 7.23 (d, 1H, J = 8.3 Hz), 7.08 (s, 1H), 6.90 (t, 1H, J = 7.7 Hz), 6.85 (d, 1H, J = 8.1 Hz), 6.18 (d, 1H, J = 7.6 Hz), 4.97 (s, 2H), 2.34 (s, 3H), 1.81–1.76 (m, 1H), 0.82–0.80 (m, 4H). ^{13}C NMR (100 MHz, DMSO- d_6): δ 171.7, 167.6, 156.8, 149.8, 148.8, 141.1, 137.1, 136.5, 130.9, 129.6, 128.7, 125.9, 120.2, 117.7, 107.7, 106.9, 104.2, 18.7, 14.5, 7.2. HRMS (ESI) m/z calculated for $\text{C}_{22}\text{H}_{23}\text{N}_6\text{O}_2$ $[\text{M} + \text{H}]^+$: 403.1882. Found: 403.2030.

N-(2-(3-Aminophenylamino)pyrimidin-5-yl)-5-(3-chlorobenzamido)-2-methylbenzamide (23). White solids. ^1H NMR (500 MHz, DMSO- d_6): δ 10.43 (s, 1H), 10.34 (s, 1H), 9.27 (s, 1H), 8.77 (s, 2H), 8.04 (s, 1H), 7.95–7.94 (m, 2H), 7.82 (d, 1H, J = 8.3 Hz), 7.67 (d, 1H, J = 8.0 Hz), 7.58 (t, 1H, J = 7.9 Hz), 7.31 (d, 1H, J = 8.4 Hz), 7.08 (s, 1H), 6.90 (t, 1H, J = 7.8 Hz), 6.86 (d, 1H, J = 8.1 Hz), 6.19 (d, 1H, J = 7.6 Hz), 4.92 (s, 2H), 2.39 (s, 3H). ^{13}C NMR (100 MHz, DMSO- d_6): δ 167.5, 164.0, 156.8, 149.9, 148.8, 141.1, 136.60, 136.57, 136.54, 133.3, 131.5, 130.9, 130.8, 130.5, 128.7, 127.3, 126.5, 125.9, 121.7, 119.2, 107.7, 107.0, 104.2, 18.8. HRMS (ESI) m/z calculated for $\text{C}_{25}\text{H}_{22}\text{ClN}_6\text{O}_2$ $[\text{M} + \text{H}]^+$: 473.1493. Found: 473.1519.

N-(2-(3-Aminophenylamino)pyrimidin-5-yl)-5-(3-(dimethylamino)benzamido)-2-methylbenzamide (24). White solids. ^1H NMR (400 MHz, DMSO- d_6): δ 10.53 (s, 1H), 10.38 (s, 1H), 9.33 (s, 1H), 8.80 (s, 2H), 8.00 (s, 1H), 7.86 (d, 1H, J = 6.7 Hz), 7.34–7.26 (m, 4H), 7.09 (s, 1H), 6.94–6.84 (m, 3H), 6.18 (d, 1H, J = 7.5 Hz), 4.97 (br s, 2H), 2.98 (s, 6H), 2.39 (s, 3H). ^{13}C NMR (100 MHz, DMSO- d_6): δ 169.5, 168.0, 158.6, 152.2, 151.7, 150.7, 143.0, 138.9, 138.1, 137.3, 132.7, 132.3, 130.8, 130.6, 127.9, 123.6, 121.2, 117.2, 117.1, 113.0, 109.5, 108.8, 106.0, 26.9, 20.8. HRMS (ESI) m/z calculated for $\text{C}_{27}\text{H}_{28}\text{N}_7\text{O}_2$ $[\text{M} + \text{H}]^+$: 482.2304. Found: 482.2508.

N-(2-(3-Aminophenylamino)pyrimidin-5-yl)-5-(3-fluorobenzamido)-2-methylbenzamide (25). White solids. ^1H NMR (400 MHz, DMSO- d_6): δ 10.44 (s, 1H), 10.38 (s, 1H), 9.32 (s, 1H), 8.77 (s, 2H), 7.95 (d, 1H, J = 2.1 Hz), 7.85–7.78 (m, 3H), 7.64–7.58 (m, 1H), 7.46 (td, 1H, J = 2.5 Hz, J = 8.8 Hz), 7.32 (d, 1H, J = 8.4 Hz), 7.08 (s, 1H), 6.90 (t, 1H, J = 7.9 Hz), 6.85 (d, 1H, J = 8.2 Hz), 6.18 (d, 1H, J = 7.6 Hz), 4.96 (s, 2H), 2.39 (s, 3H). ^{13}C NMR (100 MHz, DMSO- d_6): δ 167.6, 164.1, 163.2, 160.8, 156.8, 149.9, 148.8, 141.2, 137.0, 136.6, 131.0, 130.7, 130.6, 128.7, 125.9, 123.9, 121.7, 119.2, 118.6, 114.4, 107.8, 107.0, 104.3, 18.8. HRMS (ESI) m/z calculated for $\text{C}_{25}\text{H}_{22}\text{FN}_6\text{O}_2$ $[\text{M} + \text{H}]^+$: 457.1788. Found: 457.1844.

N-(2-(3-Aminophenylamino)pyrimidin-5-yl)-5-(3-chloro-5-(trifluoromethyl)benzamido)-2-methylbenzamide (26). White solids. ^1H NMR (300 MHz, MeOD): δ 8.73 (s, 2H), 8.24 (d, 2H, J = 11.4 Hz), 7.95 (d, 2H, J = 2.3 Hz), 7.69 (dd, 1H, J = 2.3 Hz, J = 8.3 Hz), 7.33 (d, 1H, J = 8.4 Hz), 7.23 (t, 1H, J = 2.0 Hz), 7.05 (t, 1H, J = 7.9 Hz), 6.94 (d, 1H, J = 8.1 Hz), 6.43 (d, 1H, J = 9.0 Hz), 4.63

(s, 3H), 2.47 (s, 3H). ^{13}C NMR (75 MHz, MeOD): δ 170.8, 165.6, 158.8, 152.0, 148.9, 142.2, 139.0, 137.6, 137.3, 136.7, 133.9, 133.7, 133.4, 132.6, 132.5, 130.3, 126.9, 124.1, 124.0, 121.0, 111.1, 111.0, 107.9, 19.3. HRMS (ESI) m/z calculated for $\text{C}_{26}\text{H}_{19}\text{ClF}_3\text{N}_6\text{O}_2^- [\text{M} - \text{H}]^-$: 539.1210. Found: 539.1218.

N-(2-(3-Aminophenylamino)pyrimidin-5-yl)-5-(4-chloro-3-(trifluoromethyl)benzamido)-2-methylbenzamide (27). White solids. ^1H NMR (400 MHz, DMSO- d_6): δ 10.63 (s, 1H), 10.37 (s, 1H), 9.31 (s, 1H), 8.75 (s, 2H), 8.41 (d, 1H, $J = 1.5$ Hz), 8.28 (dd, 1H, $J = 1.7$ Hz, $J = 8.4$ Hz), 7.94 (d, 1H, $J = 8.4$ Hz), 7.90 (d, 1H, $J = 2.0$ Hz), 7.82 (dd, 1H, $J = 2.0$ Hz, $J = 8.3$ Hz), 7.33 (d, 1H, $J = 8.4$ Hz), 7.07 (s, 1H), 6.89 (t, 1H, $J = 7.9$ Hz), 6.84 (d, 1H, $J = 8.2$ Hz), 6.17 (d, 1H, $J = 7.6$ Hz), 4.96 (s, 2H), 2.38 (s, 3H). ^{13}C NMR (125 MHz, DMSO- d_6): δ 167.4, 162.9, 156.8, 149.8, 148.6, 141.0, 136.5, 136.2, 133.9, 133.8, 133.2, 131.9, 130.8, 128.5, 126.8, 126.5, 125.7, 123.6, 121.7, 121.4, 119.2, 107.7, 107.0, 104.3, 18.6. HRMS (ESI) m/z calculated for $\text{C}_{26}\text{H}_{19}\text{ClF}_3\text{N}_6\text{O}_2^- [\text{M} - \text{H}]^-$: 539.1210. Found: 539.1212.

N-(2-(3-Aminophenylamino)pyrimidin-5-yl)-2-methyl-5-(4-(trifluoromethyl)benzamido)benzamide (28). White solids. ^1H NMR (400 MHz, DMSO- d_6): δ 10.60 (s, 1H), 10.39 (s, 1H), 9.36 (s, 1H), 8.78 (s, 2H), 8.18 (d, 2H, $J = 8.2$ Hz), 7.97 (d, 1H, $J = 1.8$ Hz), 7.94 (d, 2H, $J = 8.3$ Hz), 7.83 (dd, 1H, $J = 1.8$ Hz, $J = 8.3$ Hz), 7.33 (d, 1H, $J = 8.4$ Hz), 7.12 (s, 1H), 6.94–6.87 (m, 2H), 6.21 (d, 1H, $J = 7.3$ Hz), 5.22 (br s, 2H), 2.40 (s, 3H). ^{13}C NMR (100 MHz, DMSO- d_6): δ 169.4, 166.2, 158.7, 151.7, 150.1, 143.0, 140.3, 138.4, 138.3, 132.8, 132.7, 130.6, 130.4, 127.8, 127.3, 127.2, 124.4, 123.6, 121.1, 109.8, 109.2, 106.4, 20.7. HRMS (ESI) m/z calculated for $\text{C}_{26}\text{H}_{22}\text{F}_3\text{N}_6\text{O}_2^+ [\text{M} + \text{H}]^+$: 507.1756. Found: 507.1754.

N-(2-(3-Aminophenylamino)pyrimidin-5-yl)-5-cinnamamido-2-methylbenzamide (29). White solids. ^1H NMR (300 MHz, DMSO- d_6): δ 10.37 (d, 1H, $J = 3.0$ Hz), 9.41 (s, 1H), 8.77 (s, 2H), 7.87 (d, 1H, $J = 2.2$ Hz), 7.70 (dd, 1H, $J = 2.1$ Hz, $J = 8.3$ Hz), 7.65–7.56 (m, 3H), 7.47–7.40 (m, 3H), 7.27 (d, 1H, $J = 8.7$ Hz), 7.20 (s, 1H), 6.96 (d, 2H, $J = 5.0$ Hz), 6.81 (d, 1H, $J = 15.8$ Hz), 6.28 (s, 1H), 2.35 (s, 3H). ^{13}C NMR (75 MHz, DMSO- d_6): δ 168.0, 164.0, 157.1, 153.8, 150.4, 150.1, 146.0, 141.7, 140.8, 137.4, 137.0, 135.0, 131.5, 130.6, 130.3, 129.5, 129.3, 128.2, 127.8, 126.5, 122.5, 121.0, 118.4, 19.2. HRMS (ESI) m/z calculated for $\text{C}_{27}\text{H}_{25}\text{N}_6\text{O}_2^+ [\text{M} + \text{H}]^+$: 465.2039. Found: 465.2037.

N-(3-(2-(3-Aminophenylamino)pyrimidin-5-ylcarbamoyle)-4-methylphenyl)-2-naphthamide (30). White solids. ^1H NMR (400 MHz, DMSO- d_6): δ 10.56 (s, 1H), 10.40 (s, 1H), 9.34 (s, 1H), 8.79 (s, 1H), 8.62 (s, 1H), 8.11–7.89 (m, 6H), 7.88 (d, 1H, $J = 7.83$ Hz), 7.65 (s, 2H), 7.33 (d, 1H, $J = 8.4$ Hz), 7.11 (s, 1H), 6.92–6.88 (m, 2H), 6.20 (d, 1H, $J = 7.4$ Hz), 5.16 (br s, 2H), 2.40 (s, 3H). ^{13}C NMR (125 MHz, DMSO- d_6): δ 169.5, 167.4, 158.7, 151.7, 150.5, 143.0, 138.8, 138.4, 136.2, 133.9, 133.8, 132.8, 132.3, 130.8, 130.6, 129.9, 129.8, 129.7, 129.6, 128.8, 127.8, 126.2, 123.5, 120.9, 109.7, 109.0, 106.2, 20.7. HRMS (ESI) m/z calculated for $\text{C}_{29}\text{H}_{25}\text{N}_6\text{O}_2^+ [\text{M} + \text{H}]^+$: 489.2039. Found: 489.2048.

(E)-N-(2-(3-But-2-enamidophenylamino)pyrimidin-5-yl)-2-methyl-5-(3-(trifluoromethyl)benzamido)benzamide (32). White solids. ^1H NMR (400 MHz, MeOD): δ 8.76 (s, 2H), 8.27 (s, 1H), 8.21 (d, 1H, $J = 7.7$ Hz), 8.11 (s, 1H), 7.94 (s, 1H), 7.89 (d, 1H, $J = 7.7$ Hz), 7.73 (t, 1H, $J = 7.8$ Hz), 7.68 (dd, 1H, $J = 1.9$ Hz, $J = 8.3$ Hz), 7.35–7.32 (m, 2H), 7.27 (d, 1H, $J = 7.8$ Hz), 7.22 (t, 1H, $J = 8.0$ Hz), 6.91 (dt, 1H, $J = 7.0$ Hz, $J = 15.2$ Hz), 6.15 (dd, 1H, $J = 1.3$ Hz, $J = 15.2$ Hz), 2.46 (s, 3H), 1.91 (d, 3H, $J = 6.8$ Hz). ^{13}C NMR (100 MHz, MeOD): δ 170.8, 167.1, 166.7, 158.6, 152.0, 142.1, 140.3, 137.6, 137.5, 137.1, 133.6, 132.5, 132.3, 131.9, 130.7, 129.9, 129.5, 129.4, 127.3, 126.7, 125.6, 125.5, 124.1, 121.1, 116.2, 115.2, 112.2, 19.3, 17.9. HRMS (ESI) m/z calculated for $\text{C}_{30}\text{H}_{26}\text{F}_3\text{N}_6\text{O}_3^+ [\text{M} + \text{H}]^+$: 575.2018. Found: 575.2015.

(E)-N-(2-(3-(4-(Dimethylamino)but-2-enamido)phenylamino)pyrimidin-5-yl)-2-methyl-5-(3-(trifluoromethyl)benzamido)benzamide (33). White solids. ^1H NMR (400 MHz, DMSO- d_6): δ 10.57 (s, 1H), 10.41 (s, 1H), 10.02 (s, 1H), 9.62 (s, 1H), 8.81 (s, 2H), 8.32 (s, 1H), 8.28 (d, 1H, $J = 7.9$ Hz), 8.06 (s, 1H), 7.98 (d, 1H, $J = 7.8$ Hz), 7.93 (d, 1H, $J = 1.9$ Hz), 7.83 (dd, 1H, $J = 2.0$ Hz, $J = 8.3$ Hz), 7.80 (t, 1H, $J = 7.8$ Hz), 7.38–7.33 (m, 3H), 7.19 (t, 1H, $J = 8.1$ Hz),

6.73 (dt, 1H, $J = 6.1$ Hz, $J = 15.4$ Hz), 6.33 (d, 1H, $J = 15.4$ Hz), 3.17 (s, 2H), 2.39 (s, 3H), 2.26 (s, 6H). ^{13}C NMR (100 MHz, DMSO- d_6): δ 167.4, 163.8, 162.8, 156.4, 149.7, 140.8, 139.1, 136.4, 135.3, 131.7, 130.8, 130.7, 129.7, 129.2, 128.9, 128.4, 128.1, 127.0, 126.2, 125.2, 124.0, 122.5, 121.7, 119.1, 113.9, 112.5, 109.5, 59.2, 44.5, 18.7. HRMS (ESI) m/z calculated for $\text{C}_{32}\text{H}_{31}\text{F}_3\text{N}_7\text{O}_3^+ [\text{M} + \text{H}]^+$: 618.2440. Found: 618.2432.

2-Methyl-5-(3-(trifluoromethyl)benzamido)-N-(2-(3-(vinyl-sulfonamido)phenylamino)pyrimidin-5-yl)benzamide (34). White solids. ^1H NMR (400 MHz, DMSO- d_6): δ 10.57 (s, 1H), 10.42 (s, 1H), 9.92 (s, 1H), 9.68 (s, 1H), 8.81 (s, 2H), 8.33 (s, 1H), 8.28 (d, 1H, $J = 7.8$ Hz), 7.98 (d, 1H, $J = 7.9$ Hz), 7.94 (d, 1H, $J = 1.7$ Hz), 7.84 (dd, 1H, $J = 1.7$ Hz, $J = 8.2$ Hz), 7.80 (t, 1H, $J = 7.7$ Hz), 7.76 (s, 1H), 7.39 (d, 1H, $J = 8.4$ Hz), 7.34 (d, 1H, $J = 8.4$ Hz), 7.17 (t, 1H, $J = 8.2$ Hz), 6.77 (dd, 1H, $J = 9.9$ Hz, $J = 16.4$ Hz), 6.71 (d, 1H, $J = 7.9$ Hz), 6.18 (d, 1H, $J = 16.4$ Hz), 6.06 (d, 1H, $J = 9.9$ Hz), 2.39 (s, 3H). ^{13}C NMR (100 MHz, DMSO- d_6): δ 167.5, 163.9, 156.4, 149.8, 141.3, 138.0, 136.5, 136.3, 135.5, 131.8, 131.0, 130.9, 129.8, 129.4, 129.0, 128.9, 128.2, 127.6, 126.4, 124.1, 122.6, 121.8, 119.3, 113.9, 112.5, 109.6, 18.8. HRMS (ESI) m/z calculated for $\text{C}_{28}\text{H}_{24}\text{F}_3\text{N}_6\text{O}_4\text{S}^+ [\text{M} + \text{H}]^+$: 597.1532. Found: 597.1516.

N-(2-(3-(2-Chloroacetamido)phenylamino)pyrimidin-5-yl)-2-methyl-5-(3-(trifluoromethyl)benzamido)benzamide (35). White solids. ^1H NMR (400 MHz, DMSO- d_6): δ 10.58 (s, 1H), 10.43 (s, 1H), 10.25 (s, 1H), 9.70 (s, 1H), 8.82 (s, 2H), 8.33 (s, 1H), 8.28 (d, 1H, $J = 7.9$ Hz), 8.01–7.94 (m, 3H), 7.86–7.78 (m, 2H), 7.41 (d, 1H, $J = 8.1$ Hz), 7.35–7.28 (m, 2H), 7.21 (t, 1H, $J = 8.1$ Hz), 4.26 (s, 2H), 2.39 (s, 3H). ^{13}C NMR (100 MHz, DMSO- d_6): δ 167.5, 164.5, 163.9, 156.5, 149.8, 141.0, 138.6, 136.5, 135.5, 131.8, 130.9, 130.8, 129.8, 129.4, 129.0, 128.7, 128.2, 126.4, 124.2, 124.1, 121.8, 119.3, 114.3, 112.5, 109.5, 43.6, 18.8. HRMS (ESI) m/z calculated for $\text{C}_{28}\text{H}_{21}\text{ClF}_3\text{N}_6\text{O}_3^- [\text{M} - \text{H}]^-$: 581.1316. Found: 581.1323.

2-Methyl-N-(2-(3-(2-(3-oxobenzod[isothiazol-2(3H)-yl)-acetamido)phenylamino)pyrimidin-5-yl)-5-(3-(trifluoromethyl)benzamido)benzamide (36). White solids. ^1H NMR (400 MHz, DMSO- d_6): δ 10.59 (s, 1H), 10.44 (s, 1H), 10.32 (s, 1H), 9.70 (s, 1H), 8.83 (s, 2H), 8.34 (s, 1H), 8.29 (d, 1H, $J = 7.8$ Hz), 8.05 (s, 1H), 8.01–7.98 (m, 2H), 7.94 (d, 1H, $J = 1.8$ Hz), 7.91 (d, 1H, $J = 7.8$ Hz), 7.86 (dd, 1H, $J = 4.0$ Hz, $J = 8.4$ Hz), 7.81 (t, 1H, $J = 7.8$ Hz), 7.72 (t, 1H, $J = 7.2$ Hz), 7.46 (t, 1H, $J = 7.3$ Hz), 7.39 (d, 1H, $J = 8.2$ Hz), 7.34 (d, 1H, $J = 8.4$ Hz), 7.29 (d, 1H, $J = 8.2$ Hz), 7.21 (t, 1H, $J = 8.0$ Hz), 4.71 (s, 2H), 2.40 (s, 3H). ^{13}C NMR (100 MHz, DMSO- d_6): δ 167.5, 165.2, 164.9, 163.9, 156.5, 149.7, 141.4, 140.9, 138.7, 136.5, 135.4, 131.9, 131.8, 130.9, 130.8, 129.8, 129.3, 129.0, 128.7, 128.2, 126.4, 125.6, 125.3, 124.2, 124.1, 123.4, 122.6, 121.7, 119.2, 114.0, 112.3, 109.3, 46.1, 18.8. HRMS (ESI) m/z calculated for $\text{C}_{35}\text{H}_{27}\text{F}_3\text{N}_7\text{O}_4\text{S}^+ [\text{M} + \text{H}]^+$: 698.1797. Found: 698.1786.

N-(2-(3-(N-Acryloylacrylamido)phenylamino)pyrimidin-5-yl)-2-methyl-5-(3-(trifluoromethyl)benzamido)benzamide (37). White solids. ^1H NMR (500 MHz, DMSO- d_6): δ 10.89 (s, 1H), 10.60 (s, 1H), 10.24 (s, 1H), 9.13 (s, 2H), 8.32 (s, 1H), 8.28 (d, 1H, $J = 7.9$ Hz), 7.98 (d, 2H, $J = 7.0$ Hz), 7.86–7.79 (m, 2H), 7.61–7.59 (d, 2H, $J = 8.6$ Hz), 7.39–7.35 (m, 2H), 6.92 (d, 1H, $J = 8.4$ Hz), 6.44–6.24 (m, 4H), 5.78–5.75 (m, 2H), 2.40 (s, 3H). ^{13}C NMR (100 MHz, DMSO- d_6): δ 168.0, 165.6, 163.9, 163.2, 155.6, 149.3, 141.1, 139.7, 136.5, 135.8, 135.4, 132.1, 131.8, 131.6, 131.0, 130.9, 130.3, 129.7, 129.3, 128.2, 127.1, 125.2, 124.1, 124.0, 122.5, 122.1, 119.3, 18.7. HRMS (ESI) m/z calculated for $\text{C}_{32}\text{H}_{26}\text{F}_3\text{N}_6\text{O}_4^+ [\text{M} + \text{H}]^+$: 615.1968. Found: 615.2026.

N-(2-(3-(N-Acrylamidoacetamido)phenylamino)pyrimidin-5-yl)-2-methyl-5-(3-(trifluoromethyl)benzamido)benzamide (38). White solids. ^1H NMR (500 MHz, DMSO- d_6): δ 10.57 (s, 1H), 10.41 (s, 1H), 9.99 (s, 1H), 9.64 (s, 1H), 8.81 (s, 2H), 8.43 (t, 1H, $J = 5.7$ Hz), 8.33 (s, 1H), 8.28 (d, 1H, $J = 7.8$ Hz), 8.03 (s, 1H), 7.98 (d, 1H, $J = 7.8$ Hz), 7.93 (s, 1H), 7.85 (d, 1H, $J = 8.5$ Hz), 7.81 (t, 1H, $J = 7.8$ Hz), 7.37–7.33 (m, 2H), 7.27 (d, 1H, $J = 8.0$ Hz), 7.19 (t, 1H, $J = 8.1$ Hz), 6.36 (dd, 1H, $J = 10.3$ Hz, $J = 17.1$ Hz), 6.12 (d, 1H, $J = 17.0$ Hz), 5.63 (d, 1H, 10.4 Hz), 4.00 (d, 2H, $J = 5.8$ Hz), 2.39 (s, 3H). ^{13}C NMR (125 MHz, DMSO- d_6): δ 167.5, 167.3, 164.9, 163.9, 156.5, 149.8, 140.8, 138.9, 136.4, 136.3, 135.4, 131.6, 131.4, 130.8, 130.7, 129.6, 128.4, 128.1, 126.2, 125.3, 124.9, 124.0, 122.7, 121.7, 119.2,

113.8, 112.5, 109.5, 42.6, 18.6. HRMS (ESI) m/z calculated for $C_{31}H_{27}F_3N_7O_4^+$ $[M + H]^+$: 618.2077. Found: 618.2086.

N-(2-(3-Acrylamidophenylamino)pyrimidin-5-yl)-5-(3-fluorobenzamido)-2-methylbenzamide (39). White solids. 1H NMR (300 MHz, DMSO- d_6): δ 10.45 (s, 2H), 10.12 (s, 1H), 9.69 (s, 1H), 8.82 (s, 2H), 8.08 (s, 1H), 7.96 (s, 1H), 7.85–7.77 (m, 3H), 7.60 (dd, 1H, $J = 7.7$ Hz, $J = 13.6$ Hz), 7.49–7.31 (m, 4H), 7.21 (t, 1H, $J = 7.9$ Hz), 6.48 (dd, 1H, $J = 10.0$ Hz, $J = 16.9$ Hz), 6.25 (d, 1H, $J = 17.3$ Hz), 5.74 (d, 1H, $J = 10.8$ Hz), 2.38 (s, 3H). ^{13}C NMR (125 MHz, DMSO- d_6): δ 167.5, 164.0, 163.0, 162.8, 160.9, 156.5, 149.8, 140.8, 139.0, 136.8, 136.5, 132.0, 130.8, 130.6, 130.5, 128.5, 126.3, 123.7, 121.7, 119.1, 118.5, 118.3, 114.4, 114.2, 112.8, 109.7, 18.6. HRMS (ESI) m/z calculated for $C_{28}H_{23}FN_6O_3Na^+$ $[M + Na]^+$: 533.1713. Found: 533.1705.

N-(2-(3-Acrylamidophenylamino)pyrimidin-5-yl)-5-(4-chloro-3-(trifluoromethyl)benzamido)-2-methylbenzamide (40). White solids. 1H NMR (500 MHz, DMSO- d_6): δ 10.62 (s, 1H), 10.41 (s, 1H), 10.08 (s, 1H), 9.65 (s, 1H), 8.82 (s, 2H), 8.43 (s, 1H), 8.29 (d, 1H, $J = 8.4$ Hz), 8.08 (s, 1H), 7.94 (d, 1H, $J = 8.4$ Hz), 7.92 (s, 1H), 7.84 (d, 1H, $J = 8.3$ Hz), 7.39 (t, 2H, $J = 6.9$ Hz), 7.34 (d, 1H, $J = 8.3$ Hz), 7.21 (t, 1H, $J = 8.1$ Hz), 6.48 (dd, 1H, $J = 10.2$ Hz, $J = 16.9$ Hz), 6.26 (d, 1H, $J = 17.0$ Hz), 5.74 (d, 1H, $J = 10.2$ Hz), 2.40 (s, 3H). ^{13}C NMR (125 MHz, DMSO- d_6): δ 168.0, 165.5, 163.9, 163.1, 155.5, 149.2, 141.1, 139.7, 136.4, 135.8, 135.4, 132.0, 131.6, 131.5, 130.9, 130.8, 130.2, 129.6, 129.2, 128.1, 126.9, 124.0, 122.5, 122.1, 119.3, 118.2, 117.8, 18.6. HRMS (ESI) m/z calculated for $C_{29}H_{21}ClF_3N_6O_3^-$ $[M - H]^-$: 593.1316. Found: 593.1338.

N-(3-(2-(3-Acrylamidophenylamino)pyrimidin-5-ylcarbamoyl)-4-methylphenyl)-2-naphthamide (41). White solids. 1H NMR (400 MHz, DMSO- d_6): δ 10.56 (s, 1H), 10.45 (s, 1H), 10.11 (s, 1H), 9.68 (s, 1H), 8.85 (s, 2H), 8.62 (s, 1H), 8.11–8.02 (m, 6H), 7.88 (dd, 1H, $J = 1.9$ Hz, $J = 8.3$ Hz), 7.66–7.64 (m, 2H), 7.39 (d, 2H, $J = 8.0$ Hz), 7.34 (d, 1H, $J = 8.4$ Hz), 7.22 (t, 1H, $J = 8.0$ Hz), 6.50 (dd, 1H, $J = 10.1$ Hz, $J = 16.9$ Hz), 6.25 (dd, 1H, $J = 1.7$ Hz, $J = 17.0$ Hz), 5.75 (dd, 1H, $J = 1.8$ Hz, $J = 10.2$ Hz), 2.41 (s, 3H). ^{13}C NMR (100 MHz, DMSO- d_6): δ 169.5, 167.4, 164.9, 158.4, 151.7, 142.8, 141.0, 138.8, 138.4, 136.2, 133.9, 133.8, 133.7, 132.8, 132.4, 130.8, 130.5, 129.9, 129.8, 129.7, 129.5, 128.8, 128.5, 128.3, 126.2, 123.5, 121.0, 116.0, 114.6, 111.4, 20.7. HRMS (ESI) m/z calculated for $C_{32}H_{27}N_6O_3^+$ $[M + H]^+$: 543.2145. Found: 543.2126.

Biological Assays. Kinase Enzymology Assays. Kinases were purchased from Carma Biosciences. Kinase enzymology assays were performed according to the protocols specified in HTRF KinEase assays sold by Cisbio Bioassays.

Cellular Phosphorylation Assays. The assays were performed using a similar procedure as described in literature.¹⁵ 5×10^5 Ramos cells were seeded in a 12-well plate overnight. After being treated with compounds for 1 h, cells were stimulated with goat anti-human IgM antibody for 3–5 min. After centrifugation, cells were lysed by boiling in SDS buffer. Proteins were analyzed by Western blot. Data were analyzed with ImageJ and Excel.

Cell Viability Assay. Lymphoma cells were seeded in 96-well plates (5000 cells/well), incubated for 24 h, then treated with compounds for 72 h, and measured with CellTiter-Glo luminescent cell viability assay by Promega. Data analysis was performed with GraphPad Prism 5.0.

Stability Test in FaSSIF. FaSSIF solutions of compounds in a 96-well plate were incubated on a minishaker at 350 rpm at 37 °C. At each defined time point (2, 6, 10, and 24 h), samples were collected and measured with LC–MS method.

Mouse Liver Microsome Stability Study. Compounds were incubated with liver microsomes and NADPH at 37 °C. Samples were collected at different time points and centrifuged, and the supernatants were analyzed with LC–MS/MS. First-order kinetics was used to calculate $t_{1/2}$ and CL. CL^{hep} was derived from the equation $CL^{hep} = (CL)(Q)/(CL + Q)$, where Q is the estimated liver blood flow of mice at 90 mL min⁻¹ kg⁻¹. Testosterone, propranolol, and clozapine were used as positive controls.

In Vivo Pharmacokinetic Study. The pharmacokinetics of compounds 31 and 38 were evaluated in ICR mice ($n = 3$) following intravenous (iv) injection at the 1 mg/kg dose level. At various time points, blood samples were taken and analyzed by the LC–MS method.

In Vivo Pharmacodynamic Study. Female CB17/SCID mice were injected subcutaneously with 5×10^6 DoHH2 cells. When tumors reached ~ 167 mm³ on average, mice were randomized into four groups ($n = 6$ /group) and daily dosing began. Compounds were administered via tail vein as a clear solution in polyoxyl 15 hydroxystearate (Solutol)/ethanol (1:1). Tumor size and body weight were monitored periodically for 14 days. Statistical analysis was conducted using one-way ANOVA. The Dunnett test was used to analyze the statistical significance between each treatment group and the vehicle group. $P < 0.05$ is considered statistically significant. All animal studies were conducted under approved animal care protocols and AAALAC standards.

■ ASSOCIATED CONTENT

Supporting Information

Syntheses of compounds 11, 19, and 20, modeling study, and detailed procedures and data for biological assays. This material is available free of charge via the Internet at <http://pubs.acs.org>.

■ AUTHOR INFORMATION

Corresponding Author

*Phone: 86-755-26033072. E-mail: panzy@pkusz.edu.cn.

Notes

The authors declare no competing financial interest.

■ ACKNOWLEDGMENTS

Authors thank the scientists at Crown Biosciences at Beijing and Taicang, China, for their great efforts in biological assays, and Professor Junmin Quan at Peking University, China, for helpful discussions. The following financial support is gratefully acknowledged: to Z.P., Grants 2013CB910700 (973 Program), 81373270 and 21142005 (National Natural Science Foundation of China), KQTD201103, CXB201005260059A and JC201-005270281A (Shenzhen Municipal Science and Technology Innovation Council), and 20100001120030 (Ministry of Education); to N.D., Grants 81201873 (National Natural Science Foundation of China) and 7132050 (Beijing Natural Science Foundation).

■ ABBREVIATIONS USED

ABL, asbelsion murine leukemia viral oncogene; Bmx, bone marrow tyrosine kinase gene in chromosome X protein; Blk, B lymphoid tyrosine kinase; DIEA, ethyldiisopropylamine; GI_{50} , the concentration for 50% of maximal inhibition of cell proliferation; GSK3 β , glycogen synthase kinase 3 β ; HATU, (*O*-(7-azabenzotriazol-1-yl)-*N,N,N',N'*-tetramethyluronium hexafluorophosphate); HER, human epidermal growth factor receptor; HTRF, homogeneous time-resolved fluorescence; Itk, IL2-inducible T-cell kinase; Jak, Janus kinase; JNK, c-Jun N-terminal kinase; Lck, lymphocyte-specific protein tyrosine kinase; MAP2K7, dual specificity mitogen-activated protein kinase kinase 7; Nek2, “never in mitosis gene a”-related kinase 2; NIMA, never in mitosis gene a; PDGFR, platelet-derived growth factor; PLC- γ 2, 1-phosphatidylinositol 4,5-bisphosphate phosphodiesterase γ 2; Rlk, resting lymphocyte kinase; RSK, ribosomal s6 kinase; Syk, spleen tyrosine kinase; S_NAr , nucleophilic aromatic substitution

■ REFERENCES

- (1) Küppers, R. Mechanisms of B-cell lymphoma pathogenesis. *Nat. Rev. Cancer* 2005, 5, 251–262.
- (2) Nakken, B.; Munthe, L. A.; Konttinen, Y. T.; Sandberg, A. K.; Szekanecz, Z.; Alex, P.; Szodoray, P. B-cells and their targeting in

rheumatoid arthritis—current concepts and future perspectives. *Autoimmun. Rev.* **2011**, *11*, 28–34.

(3) Mohamed, A. J.; Yu, L.; Bäckerjö, C. M.; Vargas, L.; Faryal, R.; Aints, A.; Christensson, B.; Berglöf, A.; Vihinen, M.; Nore, B. F. Bruton's tyrosine kinase (Btk): function, regulation, and trans-formation with special emphasis on the PH domain. *Immunol. Rev.* **2009**, *228*, 58–73.

(4) Smith, C.; Islam, K. B.; Vořechovský, I.; Olerup, O.; Wallin, E.; Rabbani, H.; Baskin, B.; Hammarström, L. X-linked agammaglobulinemia and other immunoglobulin deficiencies. *Immunol. Rev.* **1994**, *138*, 159–183.

(5) Sideras, P.; Smith, C. I. Molecular and cellular aspects of X-linked agammaglobulinemia. *Adv. Immunol.* **1995**, *59*, 135–224.

(6) Rickert, R. C. New insights into pre-BCR and BCR signalling with relevance to B cell malignancies. *Nat. Rev. Immunol.* **2013**, *13*, 578–591.

(7) Davis, R. E.; Ngo, V. N.; Lenz, G.; Tolar, P.; Young, R. M.; Romesser, P. B.; Kohlhammer, H.; Lamy, L.; Zhao, H.; Yang, Y.; Xu, W.; Shaffer, A. L.; Wright, G.; Xiao, W.; Powell, J.; Jiang, J. K.; Thomas, C. J.; Rosenwald, A.; Ott, G.; Muller-Hermelink, H. K.; Gascoyne, R. D.; Connors, J. M.; Johnson, N. A.; Rimsza, L. M.; Campo, E.; Jaffe, E. S.; Wilson, W. H.; Delabie, J.; Smeland, E. B.; Fisher, R. I.; Braziel, R. M.; Tubbs, R. R.; Cook, J. R.; Weisenburger, D. D.; Chan, W. C.; Pierce, S. K.; Staudt, L. M. Chronic active B cell receptor signalling in diffuse large B cell lymphoma. *Nature* **2010**, *463*, 88–92.

(8) Pan, Z. Bruton's tyrosine kinase as a drug discovery target. *Drug News Perspect.* **2008**, *21*, 357.

(9) Lou, Y.; Owens, T. D.; Kuglstatter, A.; Kondru, R. K.; Goldstein, D. M. Bruton's tyrosine kinase inhibitors: approaches to potent and selective inhibition, preclinical and clinical evaluation for inflammatory diseases and B cell malignancies. *J. Med. Chem.* **2012**, *55*, 4539–4350.

(10) Mahajan, S.; Ghosh, S.; Sudbeck, E. A.; Zheng, Y.; Downs, S.; Hupke, M.; Uckun, F. M. Rational design and synthesis of a novel anti-leukemic agent targeting Bruton's tyrosine kinase (BTK), LFM-A13 [α -cyano- β -hydroxy- β -methyl-N-(2,5-dibromophenyl)propenamide]. *J. Biol. Chem.* **1999**, *274*, 9587–9599.

(11) Hantschel, O.; Rix, U.; Schmidt, U.; Bürckstümmer, T.; Kneidinger, M.; Schütze, G.; Colinge, J.; Bennett, K. L.; Ellmeier, W.; Valent, P.; Superti-Furga, G. The Btk tyrosine kinase is a major target of the Bcr-Abl inhibitor dasatinib. *Proc. Natl. Acad. Sci. U.S.A.* **2007**, *104*, 13283–13288.

(12) Di Paolo, J. A.; Huang, T.; Balazs, M.; Barbosa, J.; Barck, K. H.; Bravo, B. J.; Carano, R. A.; Darrow, J.; Davies, D. R.; DeForge, L. E.; Diehl, L.; Ferrando, R.; Gallion, S. L.; Giannetti, A. M.; Gribbling, P.; Hurez, V.; Hymowitz, S. G.; Jones, R.; Kropf, J. E.; Lee, W. P.; Maciejewski, P. M.; Mitchell, S. A.; Rong, H.; Staker, B. L.; Whitney, J. A.; Yeh, S.; Young, W. B.; Yu, C.; Zhang, J.; Reif, K.; Currie, K. S. Specific Btk inhibition suppresses B cell- and myeloid cell-mediated arthritis. *Nat. Chem. Biol.* **2011**, *7*, 41–50.

(13) Liu, L.; Halladay, J. S.; Shin, Y.; Wong, S.; Coraggio, M.; La, H.; Baumgardner, M.; Le, H.; Gopaul, S.; Boggs, J.; Kuebler, P.; Davis, J. C., Jr.; Liao, X. C.; Lubach, J. W.; Deese, A.; Sowell, C. G.; Currie, K. S.; Young, W. B.; Khojasteh, S. C.; Hop, C. E.; Wong, H. Significant species difference in amide hydrolysis of GDC-0834, a novel potent and selective Bruton's tyrosine kinase inhibitor. *Drug Metab. Dispos.* **2011**, *39*, 1840–1849.

(14) Xu, D.; Kim, Y.; Postelnek, J.; Vu, M. D.; Hu, D. Q.; Liao, C.; Bradshaw, M.; Hsu, J.; Zhang, J.; Pashine, A.; Srinivasan, D.; Woods, J.; Levin, A.; O'Mahony, A.; Owens, T. D.; Lou, Y.; Hill, R. J.; Narula, S.; DeMartino, J.; Fine, J. S. RN486, a selective Bruton's tyrosine kinase inhibitor, abrogates immune hypersensitivity responses and arthritis in rodents. *J. Pharmacol. Exp. Ther.* **2012**, *341*, 90–103.

(15) Pan, Z.; Scheerens, H.; Li, S. J.; Schultz, B. E.; Sprengeler, P. A.; Burrill, L. C.; Mendonca, R. V.; Sweeney, M. D.; Scott, K. C.; Grothaus, P. G.; Jeffery, D. A.; Spoerke, J. M.; Honigberg, L. A.; Young, P. R.; Dalrymple, S. A.; Palmer, J. T. Discovery of selective irreversible inhibitors for Bruton's tyrosine kinase. *ChemMedChem* **2007**, *2*, 58–61.

(16) Evans, E.; Ponader, S.; Karp, R.; Tester, R.; Sheets, M.; Aslanian, S.; Zhu, Z.; Chaturvedi, P.; Mazdiyasni, H.; Nacht, M.; Burger, J.; Petter, R.; Westlin, W.; Singh, J. AVL-292: a targeted therapy for Bruton's tyrosine kinase in B cell malignancies. Presented at the 16th Congress of the European Hematology Association, London, U.K., June 9–12, 2011.

(17) Kim, K.-H.; Maderna, A.; Schnute, M. E.; Hegen, M.; Mohan, S.; Miyashiro, J.; Lin, L.; Li, E.; Keegan, S.; Lussier, J.; Wrocklage, C.; Nickerson-Nutter, C. L.; Wittwer, A. J.; Soutter, H. C. N.; Han, S. K. R.; Dunussi-Joannopoulos, K.; Douhan, J., III; Wissner, A. Imidazo-[1,5-a]quinoxalines as irreversible BTK inhibitors for the treatment of rheumatoid arthritis. *Bioorg. Med. Chem. Lett.* **2011**, *21*, 6258–6263.

(18) Copeland, R. A.; Pompliano, D. L.; Meek, T. D. Drug-target residence time and its implications for lead optimization. *Nat. Rev. Drug Discovery* **2006**, *5*, 730–739.

(19) Honigberg, L. A.; Smith, A. M.; Sirisawad, M.; Verner, E.; Loury, D.; Chang, B.; Li, S.; Pan, Z.; Thamm, D. H.; Miller, R. A.; Buggy, J. J. The Bruton tyrosine kinase inhibitor PCI-32765 blocks B-cell activation and is efficacious in models of autoimmune disease and B-cell malignancy. *Proc. Natl. Acad. Sci. U.S.A.* **2010**, *107*, 13075–13080.

(20) Chang, B. Y.; Huang, M. M.; Francesco, M.; Chen, J.; Sokolove, J.; Magadala, P.; Robinson, W. H.; Buggy, J. J. The Bruton tyrosine kinase inhibitor PCI-32765 ameliorates autoimmune arthritis by inhibition of multiple effector cells. *Arthritis Res. Ther.* **2011**, *13*, R115.

(21) Aalipour, A.; Advani, R. H. Bruton tyrosine kinase inhibitors: a promising novel targeted treatment for B cell lymphomas. *Br. J. Haematol.* **2013**, *163*, 463–443.

(22) Vargas, L.; Hamasy, A.; Nore, B. F.; Smith, C. I. E. Inhibitors of BTK and ITK: state of the new drugs for cancer, autoimmunity and inflammatory diseases. *Scand. J. Immunol.* **2013**, *78*, 130–139.

(23) Sanderson, K. Irreversible kinase inhibitors gain traction. *Nat. Rev. Drug Discovery* **2013**, *12*, 649–651.

(24) Potashman, M. H.; Duggan, M. E. Covalent modifiers: an orthogonal approach to drug design. *J. Med. Chem.* **2009**, *52*, 1231–1246.

(25) Singh, J.; Petter, R. C.; Baillie, T. A.; Whitty, A. The resurgence of covalent drugs. *Nat. Rev. Drug Discovery* **2011**, *10*, 307–317.

(26) Fry, D. W.; Bridges, A. J.; Denny, W. A.; Doherty, A.; Greis, K. D.; Hicks, J. L.; Hook, K. E.; Keller, P. R.; Leopold, W. R.; Loo, J. A.; McNamara, D. J.; Nelson, J. M.; Sherwood, V.; Smail, J. B.; Trumpff-Kallmeyer, S.; Dobrusin, E. M. Specific, irreversible inactivation of the epidermal growth factor receptor and erbB2, by a new class of tyrosine kinase inhibitor. *Proc. Natl. Acad. Sci. U.S.A.* **1998**, *95*, 12022–12027.

(27) Smail, J. B.; Rewcastle, G. W.; Loo, J. A.; Greis, K. D.; Chan, O. H.; Reynier, E. L.; Lipka, E.; Showalter, H. D.; Vincent, P. W.; Elliott, W. L.; Denny, W. A. Tyrosine kinase inhibitors. 17. Irreversible inhibitors of the epidermal growth factor receptor: 4-(phenylamino)-quinazoline- and 4-(phenylamino)pyrido[3,2-d]pyrimidine-6-acrylamides bearing additional solubilizing functions. *J. Med. Chem.* **2000**, *43*, 1380–1397.

(28) Denny, W. A. Irreversible inhibitors of the erbB family of protein tyrosine kinases. *Pharmacol. Ther.* **2002**, *93*, 253–261.

(29) Liu, F.; Zhang, X.; Weisberg, E.; Chen, S.; Hur, W.; Wu, H.; Zhao, Z.; Wang, W.; Mao, M.; Cai, C.; Simon, N. I.; Sanda, T.; Wang, J.; Look, A. T.; Griffin, J. D.; Balk, S. P.; Liu, Q.; Gray, N. S. Discovery of a selective irreversible BMX inhibitor for prostate cancer. *ACS Chem. Biol.* **2013**, *8*, 1423–1428.

(30) Zhou, W.; Hur, W.; McDermott, U.; Dutt, A.; Xian, W.; Ficarro, S. B.; Zhang, J.; Sharma, S. V.; Brugge, J.; Meyerson, M.; Settleman, J.; Gray, N. S. A structure-guided approach to creating covalent FGFR inhibitors. *Chem. Biol.* **2010**, *17*, 285–295.

(31) Perez, D. I.; Palomo, V.; Perez, C.; Gil, C.; Dans, P. D.; Luque, F. J.; Conde, S.; Martinez, A. Switching reversibility to irreversibility in glycogen synthase kinase 3 inhibitors: clues for specific design of new compounds. *J. Med. Chem.* **2011**, *54*, 4042–4056.

(32) Zapf, C. W.; Gerstenberger, B. S.; Xing, L.; Limburg, D. C.; Anderson, D. R.; Caspers, N.; Han, S.; Aulabaugh, A.; Kurumbail, R.; Shakya, S.; Li, X.; Spaulding, V.; Czerwinski, R. M.; Seth, N.; Medley,

- Q. G. Covalent inhibitors of interleukin-2 inducible T cell kinase (Itk) with nanomolar potency in a whole-blood assay. *J. Med. Chem.* **2012**, *55*, 10047–10063.
- (33) Zhang, T.; Inesta-Vaquera, F.; Niepel, M.; Zhang, J.; Ficarro, S. B.; Machleidt, T.; Xie, T.; Marto, J. A.; Kim, N.; Sim, T.; Laughlin, J. D.; Park, H.; LoGrasso, P. V.; Patricelli, M.; Nomanbhoy, T. K.; Sorger, P. K.; Alessi, D. R.; Gray, N. S. Discovery of potent and selective covalent inhibitors of JNK. *Chem. Biol.* **2012**, *19*, 140–154.
- (34) Leproult, E.; Barluenga, S.; Moras, D.; Wurtz, J. M.; Winssinger, N. Cysteine mapping in conformationally distinct kinase nucleotide binding sites: application to the design of selective covalent inhibitors. *J. Med. Chem.* **2011**, *54*, 1347–1355.
- (35) Henise, J. C.; Taunton, J. Irreversible Nek2 kinase inhibitors with cellular activity. *J. Med. Chem.* **2011**, *54*, 4133–4146.
- (36) Nacht, M.; Qiao, L.; Sheets, M. P.; St Martin, T.; Labenski, M.; Mazdiyasni, H.; Karp, R.; Zhu, Z.; Chaturvedi, P.; Bhavsar, D.; Niu, D.; Westlin, W.; Petter, R. C.; Medikonda, A. P.; Singh, J. Discovery of a potent and isoform-selective targeted covalent inhibitor of the lipid kinase PI3K α . *J. Med. Chem.* **2013**, *56*, 712–721.
- (37) Cohen, M. S.; Zhang, C.; Shokat, K. M.; Taunton, J. Structural bioinformatics-based design of selective, irreversible kinase inhibitors. *Science* **2005**, *308*, 1318–1321.
- (38) Kwarcinski, F. E.; Fox, C. C.; Steffey, M. E.; Soellner, M. B. Irreversible inhibitors of c-Src kinase that target a nonconserved cysteine. *ACS Chem. Biol.* **2012**, *7*, 1910–1917.
- (39) Gushwa, N. N.; Kang, S.; Chen, J.; Taunton, J. Selective targeting of distinct active site nucleophiles by irreversible Src-family kinase inhibitors. *J. Am. Chem. Soc.* **2012**, *134*, 20214–20217.
- (40) Barf, T.; Kaptein, A. Irreversible protein kinase inhibitors: balancing the benefits and risks. *J. Med. Chem.* **2012**, *55*, 6243–6262.
- (41) Garuti, L.; Roberti, M.; Bottegoni, G. Irreversible protein kinase inhibitors. *Curr. Med. Chem.* **2011**, *18*, 2981–2994.
- (42) Dinh, M.; Grunberger, D.; Ho, H.; Tsing, S. Y.; Shaw, D.; Lee, S.; Barnett, J.; Hill, R. J.; Swinney, D. C.; Bradshaw, J. M. Activation mechanism and steady state kinetics of Bruton's tyrosine kinase. *J. Biol. Chem.* **2007**, *282*, 8768–8776.
- (43) Wahl, M. I.; Fluckiger, A.-C.; Kato, R. M.; Park, H.; Witte, O. N.; Rawlings, D. J. Phosphorylation of two regulatory tyrosine residues in the activation of Bruton's tyrosine kinase via alternative receptors. *Proc. Natl. Acad. Sci. U.S.A.* **1997**, *94*, 11526–11533.
- (44) Nisitani, S.; Kato, R. M.; Rawlings, D. J.; Witte, O. N.; Wahl, M. I. In situ detection of activated Bruton's tyrosine kinase in the Ig signaling complex by phosphopeptide-specific monoclonal antibodies. *Proc. Natl. Acad. Sci. U.S.A.* **1999**, *96*, 2221–2226.
- (45) Liu, L.; Di Paolo, J.; Barbosa, J.; Rong, H.; Reif, K.; Wong, H. Antiarthritis effect of a novel Bruton's tyrosine kinase (BTK) inhibitor in rat collagen-induced arthritis and mechanism-based pharmacokinetic/pharmacodynamic modeling: relationships between inhibition of BTK phosphorylation and efficacy. *J. Pharmacol. Exp. Ther.* **2011**, *338*, 154–163.
- (46) Kang, S. W.; Wahl, M. I.; Chu, J.; Kitauro, J.; Kawakami, Y.; Kato, R. M.; Tabuchi, R.; Tarakhovsky, A.; Kawakami, T.; Turck, C. W.; Witte, O. N.; Rawlings, D. J. PKC β modulates antigen receptor signaling via regulation of Btk membrane localization. *EMBO J.* **2001**, *20*, 5692–5702.
- (47) de Rooij, M. F.; Kuil, A.; Geest, C. R.; Eldering, E.; Chang, B. Y.; Buggy, J. J.; Pals, S. T.; Spaargaren, M. The clinically active BTK inhibitor PCI-32765 targets B-cell receptor- and chemokine-controlled adhesion and migration in chronic lymphocytic leukemia. *Blood* **2012**, *119*, 2590–2594.
- (48) Sos, M. L.; Koker, M.; Weir, B. A.; Heynck, S.; Rabinovsky, R.; Zander, T.; Seeger, J. M.; Weiss, J.; Fischer, F.; Frommolt, P.; Michel, K.; Peifer, M.; Mermel, C.; Girard, L.; Peyton, M.; Gazdar, A. F.; Minna, J. D.; Garraway, L. A.; Kashkar, H.; Pao, W.; Meyerson, M.; Thomas, R. K. PTEN loss contributes to erlotinib resistance in EGFR-mutant lung cancer by activation of Akt and EGFR. *Cancer Res.* **2009**, *69*, 3256–3261.
- (49) Vivanco, I.; Rohle, D.; Verselle, M.; Iwanami, A.; Kuga, D.; Oldrini, B.; Tanaka, K.; Dang, J.; Kubek, S.; Palaskas, N.; Hsueh, T.; Evans, M.; Mulholland, D.; Wolle, D.; Rajasekaran, S.; Rajasekaran, A.; Liao, L. M.; Cloughesy, T. F.; Dikic, I.; Brennan, C.; Wu, H.; Mischel, P. S.; Perera, T.; Mellinghoff, I. K. The phosphatase and tensin homolog regulates epidermal growth factor receptor (EGFR) inhibitor response by targeting EGFR for degradation. *Proc. Natl. Acad. Sci. U.S.A.* **2010**, *107*, 6459–6464.
- (50) Sierra, J. R.; Cepero, V.; Giordano, S. Molecular mechanisms of acquired resistance to tyrosine kinase targeted therapy. *Mol. Cancer* **2010**, *9*, 75.
- (51) Goldstein, D. M.; Kuglstatter, A.; Lou, Y.; Soth, M. J. Selective p38 α inhibitors clinically evaluated for the treatment of chronic inflammatory disorders. *J. Med. Chem.* **2010**, *53*, 2345–2353.
- (52) Liu, C.; Lin, J.; Wroblewski, S. T.; Lin, S.; Hynes, J.; Wu, H.; Dyckman, A. J.; Li, T.; Wityak, J.; Gillooly, K. M.; Pitt, S.; Shen, D. R.; Zhang, R. F.; McIntyre, K. W.; Salter-Cid, L.; Shuster, D. J.; Zhang, H.; Marathe, P. H.; Doweyko, A. M.; Sack, J. S.; Kiefer, S. E.; Kish, K. F.; Newitt, J. A.; McKinnon, M.; Dodd, J. H.; Barrish, J. C.; Schieven, G. L.; Leftheris, K. Discovery of 4-(5-(cyclopropylcarbamoyl)-2-methylphenylamino)-5-methyl-N-propylpyrrolo[1,2-f][1,2,4]triazine-6-carboxamide (BMS-582949), a clinical p38 α MAP kinase inhibitor for the treatment of inflammatory diseases. *J. Med. Chem.* **2010**, *53*, 6629–6639.
- (53) Schieven, G.; Zhang, R.; Pitt, S.; Shen, D.-R.; Cao, J.; Sack, J.; Arthur, D.; Petra, R.-M. BMS-582949 is a dual action p38 kinase inhibitor well suited to avoid resistance mechanisms that increase p38 activation in cells. *Arthritis Rheum* **2010**, *62* (Suppl. 10), S629–S630 (presented at the 2010 Congress American College of Rheumatology).
- (54) Liu, Y.; Gray, N. S. Rational design of inhibitors that bind to inactive kinase conformations. *Nat. Chem. Biol.* **2006**, *2*, 358–364.
- (55) Goldberg, D. R.; Butz, T.; Cardozo, M. G.; Eckner, R. J.; Hammach, A.; Huang, J.; Jakes, S.; Kapadia, S.; Kashem, M.; Lukas, S.; Morwick, T. M.; Panzenbeck, M.; Patel, U.; Pav, S.; Peet, G. W.; Peterson, J. D.; Prokopowicz, A. S., 3rd; Snow, R. J.; Sellati, R.; Takahashi, H.; Tan, J.; Tschantz, M. A.; Wang, X. J.; Wang, Y.; Wolak, J.; Xiong, P.; Moss, N. Optimization of 2-phenylaminoimidazo[4,5-*h*]isoquinolin-9-ones: orally active inhibitors of lck kinase. *J. Med. Chem.* **2003**, *46*, 1337–1349.
- (56) DiMauro, E. F.; Newcomb, J.; Nunes, J. J.; Bemis, J. E.; Boucher, C.; Chai, L.; Chaffee, S. C.; Deak, H. L.; Epstein, L. F.; Faust, T.; Gallant, P.; Gore, A.; Gu, Y.; Henkle, B.; Hsieh, F.; Huang, X.; Kim, J. L.; Lee, J. H.; Martin, M. W.; McGowan, D. C.; Metz, D.; Mohn, D.; Morgenstern, K. A.; Oliveira-dos-Santos, A.; Patel, V. F.; Powers, D.; Rose, P. E.; Schneider, S.; Tomlinson, S. A.; Tudor, Y. Y.; Turci, S. M.; Welcher, A. A.; Zhao, H.; Zhu, L.; Zhu, X. Structure-guided design of aminopyrimidine amides as potent, selective inhibitors of lymphocyte specific kinase: synthesis, structure–activity relationships, and inhibition of in vivo T cell activation. *J. Med. Chem.* **2008**, *51*, 1681–1694.
- (57) Kuglstatter, A.; Wong, A.; Tsing, S.; Lee, S. W.; Lou, Y.; Villaseñor, A. G.; Bradshaw, J. M.; Shaw, D.; Barnett, J. W.; Browner, M. F. Insights into the conformational flexibility of Bruton's tyrosine kinase from multiple ligand complex structures. *Protein Sci.* **2011**, *20*, 428–436.
- (58) Tsou, H. R.; Overbeek-Klumpers, E. G.; Hallett, W. A.; Reich, M. F.; Floyd, M. B.; Johnson, B. D.; Michalak, R. S.; Nilakantan, R.; Discafani, C.; Golas, J.; Rabindran, S. K.; Shen, R.; Shi, X.; Wang, Y. F.; Upeslakis, J.; Wissner, A. Optimization of 6,7-disubstituted-4-(arylamino)quinoline-3-carbonitriles as orally active, irreversible inhibitors of human epidermal growth factor receptor-2 kinase activity. *J. Med. Chem.* **2005**, *48*, 1107–1131.
- (59) Zimmermann, J.; Buchdunger, E.; Mett, H.; Meyer, T.; Lydon, N. B. Potent and selective inhibitors of the Abl-kinase: phenylamino-pyrimidine (PAP) derivatives. *Bioorg. Med. Chem. Lett.* **1997**, *7*, 187–192.
- (60) Regan, J.; Capolino, A.; Cirillo, P. F.; Gilmore, T.; Graham, A. G.; Hickey, E.; Kroe, R. R.; Madwed, J.; Moriaki, M.; Nelson, R.; Pargellis, C. A.; Swinamer, A.; Torcellini, C.; Tsang, M.; Moss, N. Structure–activity relationships of the p38 α MAP kinase inhibitor 1-(5-*tert*-butyl-2-*p*-tolyl-2*H*-pyrazol-3-yl)-3-[4-(2-morpholin-4-yl-ethoxy)naphthalen-1-yl]-urea (BIRB 796). *J. Med. Chem.* **2003**, *46*, 4676–4686.

- (61) Weisberg, E.; Manley, P.; Mestan, J.; Cowan-Jacob, S.; Ray, A.; Griffin, J. D. AMN107 (nilotinib): a novel and selective inhibitor of BCR-ABL. *Br. J. Cancer* **2006**, *94*, 1765–1769.
- (62) Huang, W.-S.; Metcalf, C. A.; Sundaramoorthi, R.; Wang, Y.; Zou, D.; Thomas, R. M.; Zhu, X.; Cai, L.; Wen, D.; Liu, S.; Romero, J.; Qi, J.; Chen, L.; Banda, G.; Lentini, S. P.; Das, S.; Xu, Q.; Keats, J.; Wang, F.; Wardwell, S.; Ning, Y.; Snodgrass, J. T.; Broudy, M. I.; Russian, K.; Zhou, T.; Commodore, L.; Narasimhan, N. I.; Mohemmad, Q. K.; Iulucci, J.; Rivera, V. M.; Dalgarno, D. C.; Sawyer, T. K.; Clackson, T.; Shakespeare, W. C. Discovery of 3-[2-(imidazo[1,2-*b*]pyridazin-3-yl)ethynyl]-4-methyl-*N*-{4-[(4-methylpiperazin-1-yl)methyl]-3-(trifluoromethyl)phenyl}benzamide (AP24534), a potent, orally active pan-inhibitor of breakpoint cluster region-abelson (BCR-ABL) kinase including the T315I gatekeeper mutant. *J. Med. Chem.* **2010**, *53*, 4701–4719.
- (63) Huang, L.; Huang, Z.; Bai, Z.; Xie, R.; Sun, L.; Lin, K. Development and strategies of VEGFR-2/KDR inhibitors. *Future Med. Chem.* **2012**, *4*, 1839–1852.
- (64) Johnson, D. S.; Weerapana, E.; Cravatt, B. F. Strategies for discovering and derisking covalent, irreversible enzyme inhibitors. *Future Med. Chem.* **2010**, *2*, 949–964.
- (65) Schwartz, P. A.; Kuzmic, P.; Solowiej, J.; Bergqvist, S.; Bolanos, B.; Almaden, C.; Nagata, A.; Ryan, K.; Feng, J.; Dalvie, D.; Kath, J. C.; Xu, M.; Wani, R.; Murray, B. W. Covalent EGFR inhibitor analysis reveals importance of reversible interactions to potency and mechanisms of drug resistance. *Proc. Natl. Acad. Sci. U.S.A.* **2014**, *111*, 173–178.
- (66) Kostwicz, E. S.; Brauns, U.; Becker, R.; Dressman, J. B. Forecasting the oral absorption behavior of poorly soluble weak bases using solubility and dissolution studies in biorelevant media. *Pharm. Res.* **2002**, *19*, 345–349.
- (67) Honigberg, L. A.; Smith, A. M.; Chen, J.; Thiemann, P.; Vernet, E. Targeting Btk in lymphoma: PCI-32765 inhibits tumor growth in mouse lymphoma models and a fluorescent analog of PCI-32765 is an active-site probe that enables assessment of Btk inhibition in vivo. *Blood*, ASH Annual Meeting Abstracts, Nov 2007; American Society of Hematology: Washington, DC, 2007; Vol. 110, p 1592.